DES HE Final Ground Risk Model

Deliverable ID:	**D3.5**
Project acronym:	**U-AGREE**
Grant:	**101167187**
Call:	**HORIZON-SESAR-2023-DES-ER-02**
Topic:	**HORIZON-SESAR-2023-DES-ER2-WA1-4**
Consortium coordinator:	**UNIVERSITAT POLITECNICA DE VALENCIA (UPV)**
Edition date:	**30 April 2026**
Edition:	**01.00**
Status:	**Official**
Classification:	**PU**

Abstract

This deliverable presents the final version of the U-AGREE Ground Risk Model, proposing targeted enhancements to the SORA ground risk framework. It introduces a physics-based, uncertainty-aware assessment of sheltering effectiveness for UAS with MTOM above 25 kg, supported by Monte Carlo simulations of building penetration. The document also quantifies obstacle effects in urban environments, demonstrating their impact on critical area reduction for both rotorcraft and fixed-wing UAS. In addition, it extends the evaluation of ground risk by introducing a structured severity assessment of environmental, economic, and reputational effects from UAS ground impacts and operations. The proposed methodologies support a more realistic and comprehensive estimation of ground risk for emerging UAS operations in complex environments.

Authoring & approval

Author(s) of the document

Organisation name	Date
EuroUSC Italia	17.04.2026

Reviewed by

Organisation name	Date
Collins Aerospace	20.04.2026
ENGage srl	20.04.2026
UPV	22.04.2026
CRIDA	29.04.2026
DLR	29.04.2026
ENAIRE	30.04.2026

Approved for submission to the SESAR 3 JU by

Organisation name	Date
Collins Aerospace	20.04.2026
ENGage srl	20.04.2026
UPV	28.04.2026
DLR	29.04.2026
ENAIRE	30.04.2026
CRIDA	30.04.2026

Rejected by[1]

Organisation name	Date

Document history

Edition	Date	Status	Company Author	Justification

[1] Representatives of the beneficiaries involved in the project.

00.01	28.11.2025	Draft	EuroUSC Italia	Table of Contents
00.02	17.04.2026	Draft	EuroUSC Italia	Finalisation of the draft
00.03	30.04.2026	Draft	EuroUSC Italia	Comments Integration
01.00	30.04.2026	Official	EuroUSC Italia	Final version of the document

U-AGREE

U-SPACE AIR AND GROUND RISK MODELS ENHANCEMENT

U-AGREE

This document is part of a project that has received funding from the SESAR 3 Joint Undertaking under grant agreement No 101167187 under European Union's Horizon Europe research and innovation programme.

Table of Contents

List of figures

List of tables

1 Executive summary

Building on the ground risk modelling framework presented in U-AGREE Deliverable D3.2 [2], this deliverable presents the proposed enhancements to the U-AGREE Ground Risk Model, addressing potential improvements of the SORA 2.5 methodology in the context of UAS operations within U-space airspace over urban environments.

The document introduces an improved, physics-based and uncertainty-aware assessment of sheltering effects, with particular focus on operations involving UAS with a maximum take-off mass above 25 kg. A probabilistic modelling approach based on Monte Carlo simulations is employed to evaluate building penetration likelihood, explicitly accounting for aircraft type, impact dynamics, material properties, and representative building typologies. This approach enables a more realistic and evidence-based evaluation of sheltering mitigation and the protection of individuals located inside structures. The results indicate that, for typical Italian building scenarios, penetration likelihood is primarily governed by the weakest elements within the building envelope—most notably windows—rather than by the overall structural strength alone.

In addition, the deliverable investigates the obstacle effect in urban environments, quantifying how the presence of buildings and other structures in general can reduce the critical area associated with UAS ground impacts. The analysis, aligned with SORA Annex F principles, demonstrates the differing applicability of this mitigation for fixed-wing and rotorcraft UAS and highlights its potential role as a complementary mitigation measure in dense urban scenarios. Analysis across various urban scenarios demonstrates that fixed-wing UAS configurations offer greater potential for employing obstacle effect mitigation strategies, particularly as a complement to other risk reduction measures.

Beyond safety outcomes directly related to crash scenarios, the document further extends the ground risk model by introducing a structured assessment of the severity of other negative effects associated with UAS ground impacts and operations. These include environmental, economic, and reputational impacts, as well as effects arising from other-than-ground-impact events such as noise, visual pollution, privacy, emissions, wildlife disturbance, and security concerns. A qualitative and quantitative scoring framework is proposed to support consistent, transparent severity assessment during the operational planning phase.

2 Introduction

2.1 Purpose and scope of the document

The purpose of this document is to present the final version of the Ground Risk Model developed within the U-AGREE project, consolidating and extending the work previously introduced in Deliverable D3.2 [2]. The document aims to address specific limitations identified in the current application of the SORA ground risk framework to emerging UAS operations, particularly in populated and urban environments. The scope of the deliverable covers three main areas.

First, it develops and applies an enhanced assessment of sheltering effects, with a particular focus on UAS operations involving UAS with a MTOM greater than 25 kg, for which existing SORA guidance requires supporting evidence. The proposed approach combines physical modelling and probabilistic Monte Carlo simulations to evaluate building penetration likelihood and to quantify the protective effect of buildings.

Second, the document investigates the obstacle effect in urban and suburban environments, analysing how the presence, density, and geometry of buildings and other obstacles influence the critical area associated with UAS ground impacts. This assessment is performed in alignment with the principles of SORA v2.5 Annex F [5] and evaluates the applicability and limitations of obstacle-based mitigation for different UAS configurations, including rotorcraft and fixed-wing aircraft.

Third, the scope is extended beyond direct safety consequences of crash scenarios by introducing a structured framework for assessing the severity of other negative effects arising from UAS ground impacts and normal operations. These effects include environmental, economic, and reputational impacts, as well as impacts related to noise, visual pollution, privacy, emissions, wildlife disturbance, and security. Both qualitative and quantitative assessment methods are proposed to support consistent severity evaluation during the operational planning phase.

On the contrary, this deliverable does not propose within its purpose and scope any improvements to the ground risk model with regard to estimating the critical area downstream of a MAC involving a manned aircraft. This decision was made because, within the SORA framework, the estimation of the critical area is associated with the ground impact phase of an UAS following a loss of control event. The critical area model adopted in this deliverable, building on the methodology presented in Deliverable D3.2 and in SORA v2.5 Annex F, does not depend on the specific initiating cause of the loss of control. In this context, events such as a MAC with a manned aircraft are addressed within the "air risk domain" of SORA. Should such an event result in an uncontrolled descent of the UAS, the subsequent ground impact is modelled using the same critical area assumptions as for other failure scenarios. As a result, the occurrence of a MAC does not, in itself, alter the critical area estimation applied in the Ground Risk Model.

2.2 Intended readership

This document is primarily intended for UAS operators, competent authorities, and regulatory bodies involved in the assessment, approval, and oversight of UAS operations under risk-based regulatory frameworks, including the SORA methodology. It is also relevant to U-space service providers, policymakers, and standardisation bodies seeking to support the safe integration of UAS into complex airspace and urban environments.

In addition, the deliverable is addressed to industry stakeholders, including UAS manufacturers, operators, and system integrators, who require quantitative and evidence-based methods to support the justification of operational mitigations, particularly for operations involving UAS with higher maximum take-off mass and operations in populated areas.

The document may further be of interest to researchers and technical experts working in the field of UAS safety, risk modelling, and urban air mobility, as it presents methodological advancements, simulation approaches, and assumptions that may support further research, validation activities, or regulatory evolution.

2.3 Background

The integration of UAS into non-segregated airspace and populated environments relies on risk-based assessment methods that are both robust and operationally applicable. In Europe, the SORA provides the accepted framework for evaluating air and ground risks of UAS operations. While SORA v2.5 offers a harmonised and pragmatic baseline, its application to emerging UAS operations in complex and urban environments might require operators to conduct complex analyses and develop supporting evidence especially if the UAS MTOM is larger than 25kg.

These limitations are increasingly relevant as current and future UAS operations may involve larger UAS, higher operational complexity, and operations closer to people and infrastructure. In particular, the assessment of sheltering and obstacle effects in the SORA ground risk model remains conservative and, in some cases, insufficiently supported by quantitative evidence. For example, the applicability of sheltering mitigation for UAS above 25 kg MTOM requires supporting evidence, but no standardised methodology is provided.

In parallel, UAS operations can generate negative effects beyond direct safety consequences from crashes, including environmental disturbance, economic loss, and reputational impact. These aspects are increasingly relevant for operational planning and societal acceptance but are not explicitly integrated into existing ground risk assessment models.

Building on the ground risk modelling framework [5] introduced in U-AGREE Deliverable D3.2 [2], this deliverable addresses these gaps by proposing targeted enhancements to the Ground Risk Model. These include a probabilistic, physics-based assessment of sheltering effectiveness for UAS with MTOM higher than 25kg, a quantitative evaluation of obstacle effects on critical area reduction in urban environments, and an extended framework for assessing the severity of negative effects from both UAS ground impacts and normal operations. Together, these enhancements aim to improve the realism, transparency, and applicability of ground risk assessment for emerging UAS operations.

For further details on the documents referenced in this section, refer to section 4 of this document.

2.4 Structure of the document

This document is arranged in the following manner:

- Section 1 provides the Executive Summary.

- Section 2 acts as an overall introduction to the matter.
- Section 3 describes the ground risk model improvements developed by U-AGREE, as well as the assumptions and parameters used in the model.
- Section 4 lists the documents referenced in the deliverable.
- Appendix A provides supporting material, including aircraft data used for simulations and detailed numerical outputs.

2.5 List of acronyms

Term	Definition
ACFR	Aircraft Critical Failure Radius
AGL	Above Ground Level
AI	Artificial Intelligence
AirMOUR	Air Mobility Urban Research
AR	Abnormal Return
ARC	Air Risk Class
ASSURE	(FAA's) Alliance for System Safety of UAS through Research Excellence
CA	Collision Avoidance
CAR	Cumulative Abnormal Return
C_d	Drag coefficient
CNPC	Control and Non-Payload Communications
CNS	Communication, Navigation, and Surveillance
ConOps	Concept of Operations
CO_2	Carbon dioxide
DES	Digital European Sky
EASA	European Union Aviation Safety Agency
ENAC	Ente Nazionale per l'Aviazione Civile (Italian Civil Aviation Authority)
EC	Economic Indicator
EM	Emissions Indicator
FAT	Fatalities
GIS	Geographic information system
GPS	Global Positioning System
HE	Horizon Europe
ICAO	International Civil Aviation Organization
iGRC	Intrinsic Ground Risk Class
JARUS	Joint Authorities for Rulemaking on Unmanned Systems
KE	Kinetic Energy

EUROPEAN PARTNERSHIP
Co-funded by the European Union

Term	Definition
MAC	Mid-Air Collision
MTOM	Maximum Take-Off Mass
mUAS	micro Unmanned Aircraft System
MUSE	Measuring U-Space Social and Environmental Impact
NASA	National Aeronautics and Space Administration
NO	Noise Indicator
PC	Privacy Indicator
PD	Probabilities of Default
RF	Relative Frequency
RR	Risk Ratio
SC	Security Categorisation
SCM	Strategic Conflict Management
SESAR	Single European sky ATM research
SESAR 3 JU	SESAR 3 Joint Undertaking
SF	Safety Factor
SORA	Specific Operations Risk Assessment
SPR	Safety, Performance and Interoperability Requirements
TLS	Target Level of Safety
UAM	Urban Air Mobility
UAS	Unmanned Aircraft System
UTM	Unmanned Traffic Management
VP	Visual Pollution Indicator
VPC	Visual Pollution Concentration
WL	Wildlife Indicator

Table 1: List of acronyms.

Co-funded by the European Union

3 Proposed improvements in the Ground Risk Model

3.1 Sheltering for UAS with MTOM above 25 kg

The Ground Risk Model in SORA includes specific provisions for the assessment of ground impact consequences. One aspect concerns the application of sheltering mitigation, which in SORA v2.5 can be claimed without additional evidence only for UAS with MTOM below 25 kg. For heavier UAS, sheltering is not excluded, but its use requires supporting evidence that is not further specified at methodological level.

The decision to focus the sheltering analysis on UAS with MTOM above 25 kg was therefore motivated by the need to explore whether this regulatory threshold reflects a physical boundary or rather a gap in available modelling approaches. As emerging UAS operations increasingly involve platforms exceeding 25 kg, this gap becomes more relevant for the applicability of the Ground Risk Model.

By extending the sheltering analysis to higher-MTOM UAS, it was investigated whether quantitative and uncertainty-aware modelling techniques can support a more informed assessment of penetration likelihood and protective effects, building on the approach already introduced in [2].

3.1.1 Extending Sheltering Mitigation to heavier UAS: Challenges and Opportunities in Urban Aerial Work Operations

3.1.1.1 Current market and SAIL restrictions

In recent years, the UAS aerial work market has expanded significantly, including applications such as goods transportation, agricultural spraying, infrastructure inspection, and the cleaning of solar panels or building façades. The effectiveness of these operations largely depends on the ability of UAS to carry meaningful payloads and to operate safely in proximity to people and infrastructure.

To meet these operational needs, manufacturers have increasingly developed UAS with a MTOM exceeding 25 kg and, in some cases, above 100 kg. These platforms are typically characterised by larger dimensions and higher potential impact energies than lighter UAS.

When applying the SORA v2.5 Ground Risk Model, UAS with MTOM in the range between 25 kg and 200 kg—generally corresponding to characteristic dimensions between approximately 1 m and 8 m—are, in many cases, constrained to operations over sparsely populated areas or controlled ground areas. This stems from the intrinsic Ground Risk Class (iGRC) determination, which increases rapidly with population density and aircraft size.

Intrinsic UAS Ground Risk Class						
Maximum UA characteristic dimension		1m / approx. 3 ft	3 m / approx. 10 ft	8 m / approx. 25 ft	20 m / approx. 65 ft	40 m / approx. 130 ft
Maximum speed		*25 m/s*	*35 m/s*	*75 m/s*	*120 m/s*	*200 m/s*
Maximum iGRC population density (people/km²)	Controlled Ground Area	1	1	2	3	3
	< 5	2	3	4	5	6
	< 50	3	4	5	6	7
	< 500	4	5	6	7	8
	< 5,000	5	6	7	8	9
	< 50,000	6	7	8	9	10
	> 50,000	7	8	Not part of SORA		

Figure 1 - Intrinsic Ground Risk Class (iGRC) determination as a function of population density and UA characteristics, source: [4]

As illustrated by the SAIL determination logic below, operations resulting in a Final GRC above 3 typically lead to SAIL III or higher.

SAIL Determination				
	Residual ARC			
Final GRC	a	b	c	d
≤2	I	II	IV	VI
3	II	II	IV	VI
4	III	III	IV	VI
5	IV	IV	IV	VI
6	V	V	V	VI
7	VI	VI	VI	VI
>7	Certified category			

Table 2: SAIL determination table [7]

In practice, most UAS operators encounter significant difficulties in complying with SAIL III and above. For example, if the Final GRC is 4, the corresponding SAIL is III, requiring the operator to obtain

Co-funded by the European Union

compliance declarations for all design-related Operational Safety Objectives (OSOs) from the UAS manufacturer. For higher Final GRC values, operations fall within SAIL IV or above, where Design Verification or Type Certification is generally required. Such certified UAS are currently not available for this class of operations.

As a consequence, the majority of current operations involving UAS above 25 kg are effectively limited to scenarios that achieve a Final GRC of 3 or lower (typically SAIL II or below). Therefore, even with the use of other mitigation measures such as parachutes, operations of UAS above 25 kg in urban areas are currently very challenging.

3.1.1.2 Market expectation and SAIL restrictions

Despite these regulatory constraints, market expectations increasingly point towards UAS operations in urban and suburban environments. In such contexts, population density can be high, yet a substantial proportion of people are protected by buildings, infrastructure, and vehicles. Although the number of people present is large, their exposure to direct ground impact risk is mitigated by sheltering.

As defined in SORA, sheltering refers to the expected protection of people in the event that a UAS crashes into a building or structure rather than directly impacting individuals. Within SORA v2.5, sheltering is treated as part of mitigation M1(A), which aims to reduce ground risk by reducing the exposure of people at risk.

Under Criterion 2 of M1(A) (*Evaluation of penetration hazard*), sheltering mitigation can be claimed without additional supporting evidence only for UAS with MTOM below 25 kg. For heavier UAS, the framework requires supporting evidence demonstrating that the aircraft is not expected to penetrate structures and fatally injure people under shelter. While examples of acceptable evidence are listed—such as testing, analysis, simulation, inspection, design review, or operational experience—no standardised methodology is provided.

This absence of a harmonised approach significantly limits the practical application of sheltering mitigation for UAS above 25 kg, particularly in urban scenarios where sheltering could otherwise play a decisive role in reducing ground risk.

3.1.1.3 Ground Risk mitigations

SORA 2.5 allows for the combined application of several ground risk mitigations, in particular M1(A), M1(B), M1(C) and M2. For the operational scenarios associated with heavier UAS, the combined use of these mitigations is especially relevant.

Mitigation M1(A) enables a reduction of the iGRC by accounting for sheltering and time-based restrictions. For UAS above 25 kg, the associated assurance criteria require supporting evidence that penetration of structures is unlikely. In this context, the assessment of penetration hazard should consider not only the characteristics of the UAS—such as mass, size, geometry, materials, and impact dynamics—but also the impact resistance of the buildings typically overflown.

Mitigation M1(B) addresses spacetime based restrictions aimed at reducing the number of people exposed on the ground, independently of sheltering. This mitigation does not introduce any aircraft specific technical challenges.

Mitigation M1(C) relies on Ground observation as a way to reduce the number of people exposed to the risk.

Mitigation M2 focuses on reducing the effects of ground impact after loss of control, either by reducing impact energy or by reducing the size of the critical area. Technologies such as parachutes primarily reduce lethality in the event of an impact with a person. However, by substantially reducing vertical velocity and kinetic energy, these systems also reduce impact severity against buildings, thereby indirectly supporting sheltering.

For urban and populated environments, the combined application of sheltering (M1(A)), spacetime restrictions (M1(B)), Ground observation (M1(C)) and impact-energy reduction (M2) can therefore support operations with UAS above 25 kg while maintaining acceptable Final GRC and SAIL levels.
Because M1(B) and M1(C) may not always apply and can create operational limits, it is crucial to quantitatively account for uncertainty when assessing penetration likelihood. The next sections describe a modelling and simulation method to support using sheltering mitigation M1(A) for UAS with MTOM over 25 kg.

3.1.2 Monte Carlo Simulation for UAS Sheltering Effectiveness

In U-AGREE Deliverable 3.2 [2], a simplified physical model was introduced to evaluate sheltering effectiveness, based on the information available in [1]. Illustrative examples were provided to demonstrate that, in certain scenarios, even UAS with a mass exceeding 25 kg may fail to penetrate some structures due to relatively low kinetic energy.

The objectives of this deliverable for the sheltering mitigation are twofold:

- Enhance the sheltering physics model originally proposed in [1], incorporating additional refinements and considerations (addressed in the subsections below); and
- Lay the foundation for a methodology capable of demonstrating that sheltering mitigation remains applicable in most situations, including operations involving UAS above 25 kg.

To address the second objective, two approaches were considered:

- **Deterministic calculations**: this method relies on detailed input data – such as mass, drag coefficient, surface area, and precise building material properties – to assess sheltering effectiveness. The main limitation of this approach is the current lack of sufficiently accurate data.
- **Probabilistic modelling**: This approach estimates sheltering effects under uncertainty using a Monte Carlo simulation technique. Monte Carlo techniques are used to quantify the effect of uncertainty and variability in complex systems where outcomes depend on many uncertain inputs. Instead of relying on a single “worst-case” or “average” scenario, they estimate probabilities and distributions of outcomes by repeatedly simulating the system under many plausible realizations of the input parameters. The goal is to demonstrate that, even with significant data variability, sheltering remains applicable in most cases for the majority of UAS expected to operate under Specific Category authorizations in the near future.

The adoption of the Monte Carlo approach is driven by the presence of multiple sources of uncertainty affecting both UAS characteristics and building material properties. These uncertainties cannot be adequately captured through by single deterministic values, as their combined influence on outcomes may be non-linear. Monte Carlo simulation enables the propagation of these uncertainties, providing a robust statistical characterization of sheltering effectiveness. This method is widely applied in aviation safety and trajectory prediction, including UAS Safety assessments (see example in [3]).

For the reasons outlined above, the second approach was selected and implemented through a Python-based algorithm, which performs the calculations as follows:

1. **Input selection**: the user specifies:
    - The MTOM;
    - the number of simulations to be performed;
    - the building "material mix" to be tested (refer also to section 3.1.2.5); and
    - proportion of rotorcraft and fixed-wing aircraft to simulate;
2. **Aircraft type assignment**: for each simulation run, the aircraft type (rotorcraft or fixed-wing) is randomly assigned according to the user-defined distribution provided at input level. Simulations can also be restricted to rotorcraft-only or fixed-wing-only configurations. Further details are provided in Section 3.1.2.1.
3. **Frontal area estimation**: the algorithm estimates the aircraft frontal area as described in section 3.1.2.2.
4. **Drag coefficient selection**: For rotorcraft configurations, a drag coefficient is randomly sampled from predefined ranges consistent with representative rotorcraft geometries (see section 3.1.2.3).
5. **Impact kinetic energy calculation**: using the previously derived parameters, the algorithm computes the unmanned aircraft impact kinetic energy:
    - For rotorcraft: a ballistic descent model is applied; and
    - For fixed-wing aircraft: a glide or cruise descent model coherent with SORA v2.5 assumptions is used.

    Further details are provided in section 3.1.2.4.
6. **Building material selection**: At each simulation iteration, the algorithm randomly selects the impacted building material according to a user-defined material mix specified at input level. The material mix defines both the set of material typologies to be considered and their associated probabilities of impact, representing the likelihood of striking one material rather than another (for example `material_mix = {"Reinforced concrete 100 mm - roof": 30,"Unreinforced Brick - wall": 56,"Plywood siding - wall": 14}` represents a scenario in which, for each simulated impact, there is a 30% probability of striking a reinforced-concrete roof element, a 56% probability of striking an unreinforced brick wall, and a 14% probability of striking a plywood siding wall). For the selected material, the maximum kinetic energy absorbable by the structure without penetration is then computed (see also section 3.1.2.5 for more details).
7. Penetration is assessed by evaluating the net kinetic energy of the impact:

$$KE_{net} = KE_{aircraft} - KE_{absorbed}$$

Where:

- $KE_{aircraft}$ is the UA's impact kinetic energy;
- $KE_{absorbed}$ is the maximum kinetic energy absorbable by the impacted structure without penetration occurrence; and
- KE_{net} is the net kinetic energy of a UA impact into a structure.

If $KE_{net} < 0$, penetration does not occur.

By running a sufficiently large number of simulations, the model shall enable a probabilistic assessment of penetration likelyhood and demonstrate that, up to a given MTOM threshold, penetration is unlikely to occur in a significant proportion of cases.

3.1.2.1 Considerations on aircraft type selection

The first step of the Monte Carlo simulation consists of the random assignment of an aircraft type from a predefined set of UAS categories. This distinction is required because different aircraft types exhibit significantly different impact dynamics.

The simulations can be executed considering:

- rotorcraft only,
- fixed-wing aircraft only; or
- a mixed fleet composed of both rotorcraft and fixed-wing.

To define a representative fleet mix for the mixed-fleet scenario, the Italian operational context is adopted as a reference. This choice is based on the authors' direct operational experience with UAS and on the availability of national fleet data.

To ensure that the simulation reflects the expected composition of UAS operating in Italian airspace, data published by ENAC have been used [24].

Based on ENAC-authorized UAS in the Specific category (Italy, updated 17/12/2025), the fleet mix for UAS weighing between 25 and 200 kg consists of approximately 84.4% rotorcraft and 15.6% fixed-wing aircraft. For modelling purposes, these values are approximated to 85% and 15% in the subsequent simulations.

While this fleet distribution provides a reasonable first-order approximation, it does not account for differences in exposure time. Although rotorcraft dominate in terms of number of authorized operations, their typical flight durations are generally shorter than those of fixed-wing aircraft. As a result, a fleet mix weighted purely by aircraft count may underrepresent the effective exposure of fixed-wing operations. Incorporating exposure time into the fleet mix definition is therefore identified as an area for future refinement, with the objective of improving the representativeness and accuracy of the impact risk assessment.

3.1.2.2 Frontal Area estimation

The main challenge in setting up the Monte Carlo simulation lies in defining appropriate ranges of values that are representative of the frontal area (A) with which the UAS impacts the structure and in establishing a possible correlation between these areas and the MTOM assigned to the aircraft.

At first glance, one might consider relying on geometric similarity arguments, based on the following rationale:

- The MTOM of an aircraft scales with its volume, and therefore with the cube of a characteristic length ($MTOM \propto L^3$); and
- The frontal Area (A) scales with the square of the same characteristic length ($A \propto L^2$).

Combining these relationships leads to a bounding relationship between MTOM and frontal area of the form:

$$A = k \cdot MTOM^{2/3}$$

where k is a configuration-dependent coefficient that captures differences in aircraft geometry, in particular between rotorcraft and fixed-wing designs.

However, inspection of the empirical data reported in Table 33 shows that:

- The direct correlation between MTOM and frontal area is relatively weak, whereas
- A stronger and more physically meaningful correlation is observed between the maximum characteristic dimension of the UA and the frontal area, especially for rotorcraft.

Model	Aircraft type	MTOM [kg]	Characteristic dimension [m]	Frontal Area [m^2]
DJI Agras T100	rotorcraft	175	3.91 (tip-to-tip diagonal)	0.33
DJI Agras T50	rotorcraft	103	3.57 (tip-to-tip diagonal)	0.21
DJI Agras T25	rotorcraft	58	3.20 (tip-to-tip diagonal)	0.23
DJI FlyCart 30	rotorcraft	95	3.58 (tip-to-tip diagonal)	0.26
Flying Basket FB3	rotorcraft	115	2.97 (tip-to-tip diagonal)	0.13
DJI Agras T30	rotorcraft	76.5	3.92 (tip-to-tip diagonal)	3.92
TEKEVER AR5	Fixed-wing	150	7.3 (wingspan)	0.24
Rigitech ER-03	Fixed-wing	21	2.68 (wingspan)	0.05
Germandrones Songbird	Fixed-wing	14	2.98 (wingspan)	0.02
Milvus Tesi S.r.l.	Fixed-wing	65	4.8 (wingspan)	0.23
FoxTech Ayk 350	Fixed-wing	35	3.5 (wingspan)	0.08

Table 3: Frontal area data for a set of rotorcraft and fixed wing aircraft, source: datasheet/Flight Manuals

This observation is also reflected in the approach adopted by the UK CAA for sheltering in its proposed Amendment to AMC and GM for [25], which proposes a classification table that correlates frontal area directly with the characteristic dimension of the unmanned aircraft (table 4).

Wingspan (m)	1	3	8	20	40
Frontal area (m^2)	0.1	0.5	2.5	12.5	25

Table 4: Frontal area vs wingspan, source [25]

Given that the present study is restricted to UAS with an MTOM between 25 kg and 200 kg, a conservative assumption can be made whereby the frontal area is considered to lie within the range:

$$A \in [0.1, 0.5]\ m^2$$

This range is considered applicable to both fixed-wing and rotorcraft. Should a broader and more representative dataset become available, the assumed parameter ranges could be further refined, enabling a reduction in modelling uncertainties and an overall improvement in the robustness and fidelity of the results.

3.1.2.3 Drag coefficient estimation

The drag coefficient (C_d) is a dimensionless parameter that quantifies the aerodynamic resistance encountered by an object as it moves through the air.

According to the SORA Annex F [5], the typical range of drag coefficients relevant for ballistic descent is discussed in section A.3.6 from Annex F. It is noted that, for most objects, C_d generally falls between 0.2 (representing very streamlined shapes) and 1.2 (representing highly non-aerodynamic or bluff bodies). For a ballistically descending aircraft, it is unlikely that the drag coefficient would be at the lower end of this range, as such objects are rarely streamlined during descent. Conversely, selecting a value at the upper end would yield more optimistic (i.e., lower) impact speeds due to increased drag.

In Monte Carlo sheltering simulations, for rotorcrafts, the full range of 0.2 to 1.2 for the drag coefficient is used. This range is sampled according to a uniform distribution to account for the inherent uncertainty in the actual aerodynamic configuration during descent.

3.1.2.4 Modelling Descent Dynamics: Ballistic Drop and Glide/Cruise Descent

UAS exhibit significantly different impact dynamics depending on their configuration—rotorcraft (e.g., multirotors) versus fixed-wing platforms. SORA Annex F [5] (section A.2.1) highlights the importance of defining realistic ranges for both impact speed and angle, tailored to the aircraft type.

Section A.2.3 of Annex F identifies three representative descent scenarios:

- **Scenarios 1** and **2**: Glide and cruise descent, where the aircraft retains some lift through aerodynamic surfaces (typical for fixed-wing platforms).

- **Scenario 3**: Ballistic or near-ballistic descent, primarily relevant for rotorcraft that have lost lift and descend under gravity and aerodynamic drag.

For fixed-wing platforms, glide or cruise descent scenarios are generally more representative than ballistic descent. Fixed-wing failures typically occur in two ways:

- Engine-out with control surfaces active, leading to a glide descent.
- Catastrophic failure during powered flight, resulting in a cruise impact.

According to Annex F (Section A.2.3), the following assumptions apply:

- **Glide descent:** Impact angle ≈ **10°**, $v_{impact} \approx \mathbf{0.65 \times v_{max}}$
- **Cruise descent:** Impact angle ≈ **35°**, $v_{impact} \approx \mathbf{v_{max}}$

Where v_{impact} is the velocity at which the fixed wing aircraft would impact the building, while the $v_{\max}$ is the aircraft maximum groundspeed.

Therefore, to model these scenarios the code:

1. Randomly selects a descent scenario between glide and cruise with equal probability.[2]
   a. If the scenario selected is glide: set impact angle = 10° and calculate the impact speed as $v = 0.65 \cdot v_{max}$
      i. v_{max} is sampled uniformly in the interval [25, 47] m/s. The interval has been determined using the data reported in 0 of the present document.
   b. If the scenario selected is cruise, set impact angle = 35° and calculate the impact speed as $v = v_{max}$
      i. v_{max} is sampled uniformly in the interval [25, 47] m/s. The interval has been determined using the data reported in 0 of the present document.

For ballistic descent—characteristic of rotorcraft in loss-of-lift situations—Section 4.3.1 of [2] provides a simplified formula for estimating the terminal velocity:

$$V_{term} = \sqrt{\frac{2 \cdot MTOM \cdot g}{\rho \cdot A \cdot C_d}}$$

Where $MTOM$ is the aircraft mass, g is the gravitational acceleration, ρ is the air density, A is the frontal area and C_d is the drag coefficient. However, to improve accuracy beyond this simplified approach, the JARUS "Quantitative Methods" subgroup (WG6) developed the Casex Python package, which offers user-friendly tools for operators and authorities. The class `BallisticDescent2ndOrderDragApproximation` within Casex computes impact speed and angle for rotorcraft during ballistic descent using a second order drag model. This method provides a closed-form solution—avoiding numerical integration—while maintaining fidelity to real-world descent dynamics, as described in [6].

To calculate impact velocity and angle, the following parameters are required:

- **Altitude AGL at the start of the fall**: Sampled from a uniform distribution in the range [3, 120] m. The upper limit reflects operational constraints in the Open and Specific categories, which typically cap altitude at 120 m to minimize conflict with manned air traffic.

---

[2] This represents an initial assumption adopted for the purpose of setting up the simulation. More detailed statistical data on the relative likelihood of the different scenarios would be required to more accurately represent the behaviour of fixed-wing aircraft.

Co-funded by the European Union

- **Initial horizontal velocity ($v_{x,i}$)**: Derived from UAS manufacturer specifications (see 0). Sampled uniformly within [14, 32] m/s.
- **Initial vertical velocity ($v_{y,i}$)**: Also based on manufacturer data. Sampled uniformly within [-5, 5] m/s (see 0).

Both for glide/cruise (fixed wing) and ballistic descent (rotorcraft), the outputs to obtain the penetration check are **impact angle** and **impact speed**.

The impact speed will be used to conservatively estimate the aircraft's kinetic energy, assuming that the entire kinetic energy is transferred to the structure. The calculation follows the classical formula:

$$KE_{aircraft} = \frac{1}{2}mv^2$$

3.1.2.5 Computation of the Energy Absorbed by the structure impacted

The estimate of the energy absorbed by the impacted structure follows the methodology and data already reported in [2], derived from [1]. When a structure providing shelter deforms, fractures, and undergoes displacement under aircraft impact, it can absorb part of the aircraft's kinetic energy without being penetrated. The energy absorption characteristics adopted in this work come from experimental campaigns in which explosive projectiles (spherical sabot rounds) impacted representative wall and roof specimens at calibrated kinetic energy levels. The corresponding roof and sidewall performance values are reported in Table 5: Roof Kinetic Energy Absorption Values and Table 6: Side Wall Kinetic Energy Absorption Values

Roof Type	**KE absorbed by roof (ΔKE_n) in J**
10.16 cm Reinforced Concrete	13560
35.56 cm Reinforced Concrete	271164
Plywood/ Wood Joist (5x25 cm at 40.64 cm)	68
Gypsum/ Fiberboard/Steel Joist	34
Plywood Panelized (5x15 cm at 61 cm)	68
5 cm lightweight Concrete/ Steel Deck and Joists	2712
Medium Steel Panel (18 gauge)	2034
Light Steel Panel (22 gauge)	1356
Steel (automobile)	271

Table 5: Roof Kinetic Energy Absorption Values

Wall Type	KE absorbed by roof (ΔKE_n) in J
Steel Siding (22 Gauge)	1356
20.32 cm unreinforced CMU (Concrete Masonry Unit)	678
20.32 cm reinforced CMU	678
20.32 cm reinforced Concrete	67791
35.56 cm reinforced Concrete	271164
15.24 cm reinforced Concrete Tilt-Up	50844
1.27 cm Plywood Siding	136
20.32 cm unreinforced brick	13559
Steel (automobile doors)	1356

Table 6: Side Wall Kinetic Energy Absorption Values

The kinetic energy parameter ΔKE_n shown in the tables is defined as the average kinetic energy per unit impactor area. At the conclusion of the impact testing, the impact areas from all rounds were averaged to obtain the average cross sectional area of $\sim 0.005\ m^2$.

The absorbed KE can then be estimated as:

$$KE_{absorbed} = \frac{A_{CrossSection}}{A_{ScalarConstant}} \cdot \Delta KE_n$$

Where:

- $A_{CrossSection}$ is the frontal area of the UA
- $A_{ScalarConstant}$ is the average cross sectional area of $\sim 0.005\ m^2$ mentioned above, and
- $KE_{absorbed}$ is the maximum KE that the structure can absorb without penetration occurrence.

This approach is most accurate when the aircraft cross section involved in the impact is of the same order of magnitude as the experimental impactor. When extrapolated to larger aircraft, the assumption of a single scalar absorption factor may introduce additional uncertainty. Nevertheless, the three study cases reported in Section 4.12.3 of [1] show that the test data can still provide a useful indication of the level of protection offered by sheltering to occupants, including for larger aircraft.

To simulate realistic scenarios, the material categories in Table 55 and Table 66 must be mapped to representative real world construction solutions. The tabulated items do not describe detailed building stratigraphies; rather, they provide impact and penetration resistance categories. Therefore, real buildings should be mapped to material archetypes with equivalent impact behaviour, in a way that is realistic and consistent with the dominant construction technologies and with the presence of load bearing structural elements.

This approach is consistent with that adopted in [25]. In particular, [25] (addressing amendments proposed by the UK Civil Aviation Authority) presents a methodology to assess the applicability of sheltering based mitigation measures, building on the study in [1]. Table B3 of [25] shows a material mapping for the UK context, reproduced below:

Building Description	Representative Roof for Penetration Analysis	Representative Wall for Penetration Analysis
UK residential home clay or slate tiled roof, non-flat	8 inch unreinforced brick	Plywood Panelised
UK residential home (built pre 1950 but post 1900)	8 inch CMU	Steel Joist
Caravan/ Trailer/ Temporary office trailer	Half inch Plywood siding	Steel Joist
Small commercial buildings and public buildings like hospitals, council buildings	6 inch reinforced concrete	2 inch light weight concrete or steel deck
Large apartment complex / large commercial buildings	8 inch reinforced concrete	22 gauge steel roof with 3 inch to 4 inch concrete
Warehouses	Steel sliding	Light steel panel
Village houses constructed before 19th century	Half inch Plywood siding	Gypsum
Wooden houses	Half inch Plywood siding	Plywood Panelised
Festival and/or concert tents (indoor)	No walls	Gypsum or lower
Glass roofing (conservatories)	Half inch plywood sliding or lower	Gypsum or lower

Table 7: UK Scenario

A comparable mapping exercise can be performed for buildings in other European Union Member States, provided that appropriate and authoritative data sources are used.

As an illustrative example, an initial attempt has been made to map Italian residential buildings—selected due to the author's familiarity with the national building stock, though the approach is in principle transferable to other EU countries—using data from the TABULA and EPISCOPE projects [26] (refer also to https://webtool.building-typology.eu/#bm, which provides information about type of construction for roofs and walls for buildings with different characteristics, divided by year of construction). By analysing the data provided by the sources mentioned above, the following "qualitative mapping" can be carried out for residential buildings:

Building Description	Typical Roof Construction	Representative Roof for Penetration Analysis	Typical Wall Construction	Representative Wall for Penetration Analysis
Residential scenario: • Single Family Houses • Multifamily Houses • Small condominiums/ townhouses	• Brick-concrete composite (latero-cemento) slabs • Masonry/ clay tile covering	Reinforced Concrete Roof / RC slab	• Hollow-brick cavity walls • Reinforced Concrete structural frame + brick infill	Unreinforced brick wall or RC wall or masonry wall

Building Description	Typical Roof Construction	Representative Roof for Penetration Analysis	Typical Wall Construction	Representative Wall for Penetration Analysis
• Small apartment buildings				

Table 8: Residential scenario for Italy

Residential buildings were mapped to representative wall and roof resistance classes based on their dominant load-bearing construction. Roofs characterized by latero-cement composite slabs with clay tile coverings were mapped to reinforced concrete roof classes, as the structural response is governed by the RC slab rather than the non-structural roofing elements. For vertical structures, single-family houses and townhouses with masonry cavity walls were mapped to masonry wall classes. Multi-family and small apartment buildings characterized by reinforced concrete frames with brick infill walls were mapped to reinforced concrete wall classes.

Compared to a suburban or residential contexts, an urban scenario typically introduces:

- Higher building density
- Greater building height
- More heterogeneous construction types
- A higher proportion of non-residential buildings

Within this context, it is clear that the prevalence of reinforced concrete and steel-based structures increases.

Building Description	Typical Roof Construction	Representative Roof for Penetration Analysis	Typical Wall Construction	Representative Wall for Penetration Analysis
Urban scenario: • Large office buildings • Shopping malls • Large Apartment buildings	• RC slabs	Reinforced Concrete Roof / RC slab	• Hollow-brick cavity walls • Reinforced Concrete structural frame + brick infill	Unreinforced brick wall or RC wall

Table 9: Urban scenario for Italy

A more detailed evaluation can be carried out by considering a specific scenario in which an UA impacts a single building with defined characteristics. As a case study, an Italian multifamily house (MFH) of approximately three stories, built in the 1946–1980 period, can be considered. In Italy, this is among the most common residential building types, widely represented in the existing building stock and prevalent in urban and peri urban areas. This building type typically presents the characteristics summarised below:

Building element	Typical Construction	Representative Roof for Penetration Analysis
Roof	Ceiling with reinforced brick-concrete slab	Reinforced Concrete Roof
Wall	Solid brick masonry	Unreinforced brick wall
Windows	Single glass window/ window glazing	Gypsum (as derived from Table 7: UK Scenario)

Table 10: Typical materials for an Italian MFH, 1946-1980

Building	MFH house of 1946-1980 (approx. 3 floors)
Typical roof area (A_{roof})	320 m^2
Typical wall area (A_{wall})	779.7 m^2
Typical windows area (A_{window})	149.6 m^2 (Windows-to-wall ratio of approx.. 16%)

Table 11: Typical surface area characteristic of a standard Italian MFH, source: [28]

Another aspect to consider is the probability of impacting the roof, a wall, or a window in the event of a UAS crash. As a first approximation, if the aircraft is operating above the building (a plausible assumption for a relatively low building in this case study), a multirotor terminated by a flight termination system (FTS) is more likely to strike the roof than a side wall or a window, because it is typically characterised by steeper impact angles (approximately 50–90° with respect to the ground, as derived from Section A.2.1 of [5]). Conversely, a fixed wing aircraft may impact a building with a shallower angle (approximately 35° in cruise and approximately 10° in glide), making it more likely to strike side walls or windows.

Aircraft type	Impact angle ϑ (from horizontal)	Impacted building	Probability of hitting roof	Probability of hitting wall	Probability of hitting window
Multirotor	60 deg assumed	MFH with the characteristics reported in **Error! Reference source not found.**	0.37	0.53	0.10
Fixed-wing	22.5 deg assumed	MFH with the characteristics reported in Table 9	0.12	0.73	0.14
Fleet mix 85% multirotor, 15 % fixed wing	54.4 deg assumed	MFH with the characteristics reported in Table 9	0.32	0.57	0.11

Table 12: Probabilities difference for different scenarios

An important observation concerns impacts on windows. The extent of damage to glass depends heavily on the type of glass: for example, one could consider standard glass, tempered glass, laminated glass or double or triple-glazed units. Document [1] does not provide experimental results specifically addressing window impacts; therefore, the simulation assumes that windows have kinetic energy parameters comparable to gypsum (as derived from [25]). It is important to note, however, that as also observed in [1], "*There are also impact standards for architectural glazing, but the examined KE levels are similarly small compared to those relevant to mUAS*". This suggests that many UAS, including some below 25 kg MTOM, could penetrate buildings when impacting windows.

It would also be interesting to evaluate how building density influences the representative material mix outlined above. Intuitively, a more compact urban environment, both for multirotor and fixed wing aircraft, reduces the likelihood of striking side walls or windows rather than roofs; however, this is beyond the scope of the present deliverable.

3.1.3 Sheltering simulations results

3.1.3.1 Case study 1 – rotorcraft only:

In Case Study 1, the sheltering effect associated with a fleet mix composed exclusively of multirotor UAS is evaluated. For the purposes of this assessment, a representative material mix consistent with a typical Italian multi-family residential building has been adopted (see sec. 3.1.2.5 for additional details). The assumed distribution of building elements and corresponding representative materials used for the analysis is summarised in **Error! Reference source not found.**

Building element	Representative material for penetration analysis	Percentage % (considering an average impact angle of 60 deg)
Roof	Reinforced concrete 100 mm - roof	37
Wall	Unreinforced Brick - wall	53
Windows	Gypsum/ fiberboard/ steel joist – roof (as derived from Table 7: UK Scenario, Window glazing/ glass may be assimilated to gypsum or lower for representativeness)	10

Table 13: material mix for Case study 1

Monte Carlo simulations were performed using $N = [1000,\ 10000, 100000]$ trials. The analysis covered a range of maximum take-off mass (MTOM) values, namely MTOM = [5, 10, 15, 20, 25, 50, 75, 100, 125, 150, 175, 200] kg.

The resulting median (50th percentile) values of:

- aircraft kinetic energy versus MTOM,

- net kinetic energy versus MTOM, and
- probability of penetration versus MTOM

are presented in **Error! Reference source not found.**2 (a), (b), and (c), respectively. A complete set of simulation outputs is provided in Appendix 0 for reference.

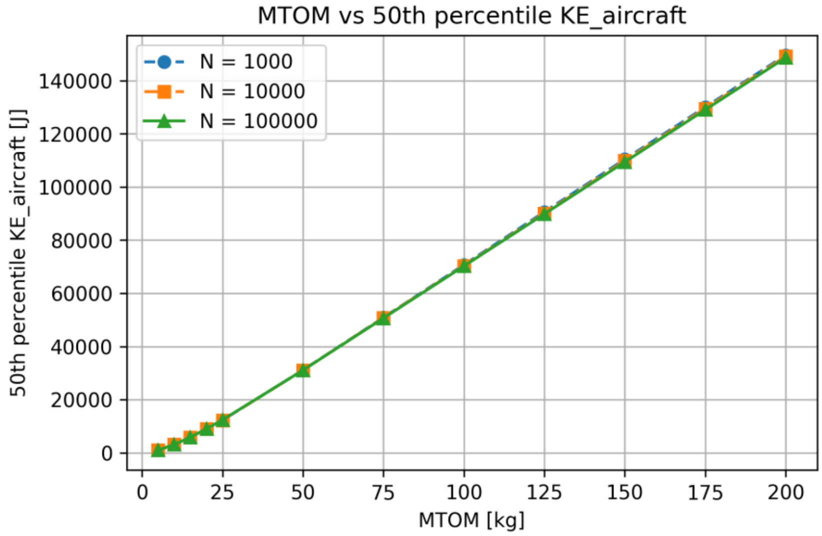

(a) The figure shows the median value of the estimated aircraft KE. A clear linear increase in the 50th-percentile aircraft KE with increasing aircraft mass can be observed.

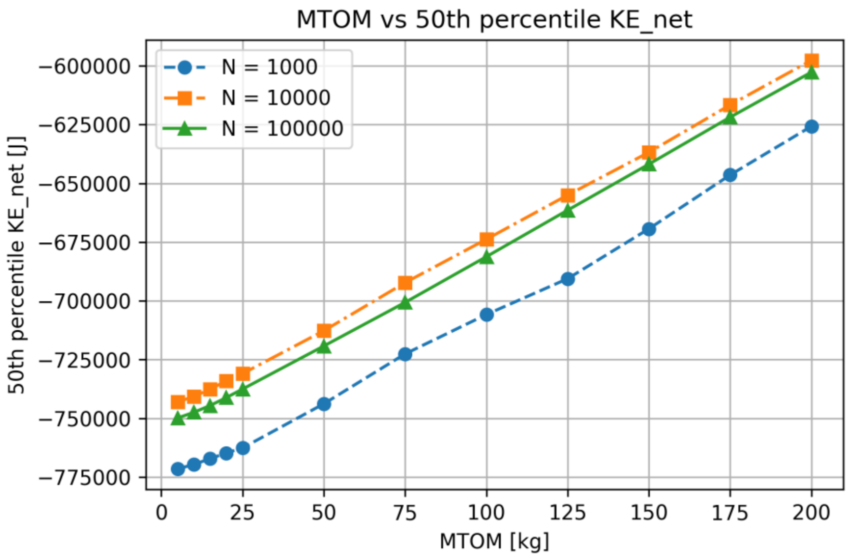

(b) This figure shows the median value of the difference between the aircraft kinetic energy (KE) and the maximum energy absorbable by the building. A clear linear trend of the KE difference with respect to MTOM can also be observed. The median (50th-percentile) value remains consistently negative over the entire MTOM range—ranging approximately from −775 kJ to −600 kJ—which is consistent with the fact that, in the majority of simulated cases, building penetration does not occur.

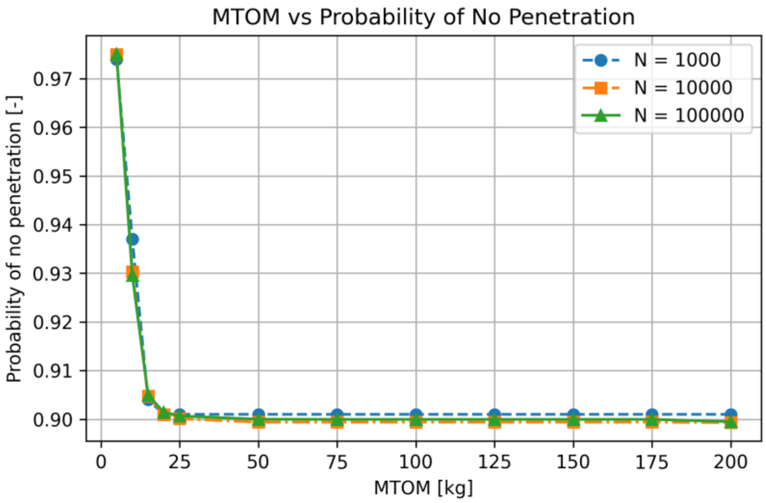

(c) This graph shows the probability of not penetrating a building versus the aircraft MTOM, one could observe that, for smaller aircraft (5 kg MTOM), we start from a probability of no penetration of 98%, which drops significantly until a plateau is reached around 25 kg. After this limit, the probability of no penetration remains around 90%. This result indicates that the probability of non penetration is driven by the most fragile element (namely, the glass from which the windows are made).

Figure 2 - plots of results obtained for Case Study 1

3.1.3.2 Case study 2 – fixed-wing only:

In Case Study 2, the sheltering response associated with a fleet mix composed exclusively of fixed-wing UA is evaluated. For the purposes of this assessment, a representative material mix consistent with a typical Italian multi-family residential building has been adopted (see sec. 3.1.2.5 for additional details). The assumed distribution of building elements and corresponding representative materials used for the analysis is summarised in **Error! Reference source not found.**

Building element	Representative material for penetration analysis	Percentage % (considering an average impact angle of 22.5 deg)
Roof	Reinforced concrete 100 mm - roof	13
Wall	Unreinforced Brick - wall	73
Windows	Gypsum/ fiberboard/ steel joist – roof (as derived from Table 7: UK Scenario, Window glazing/ glass may be assimilated to gypsum or lower for representativeness)	14

Table 14: material mix for Case Study 2

Monte Carlo simulations were performed using $N = [1000,\ 10000, 100000]$ trials. The analysis covered a range of maximum take-off mass (MTOM) values, namely MTOM = [5, 10, 15, 20, 25, 50, 75, 100, 125, 150, 175, 200] kg.

The resulting median (50th percentile) values of:

- aircraft kinetic energy versus MTOM,
- net kinetic energy versus MTOM, and
- probability of penetration versus MTOM

are presented in Figure 3 (a), (b), and (c), respectively. A complete set of simulation outputs is provided in Appendix 0 for reference.

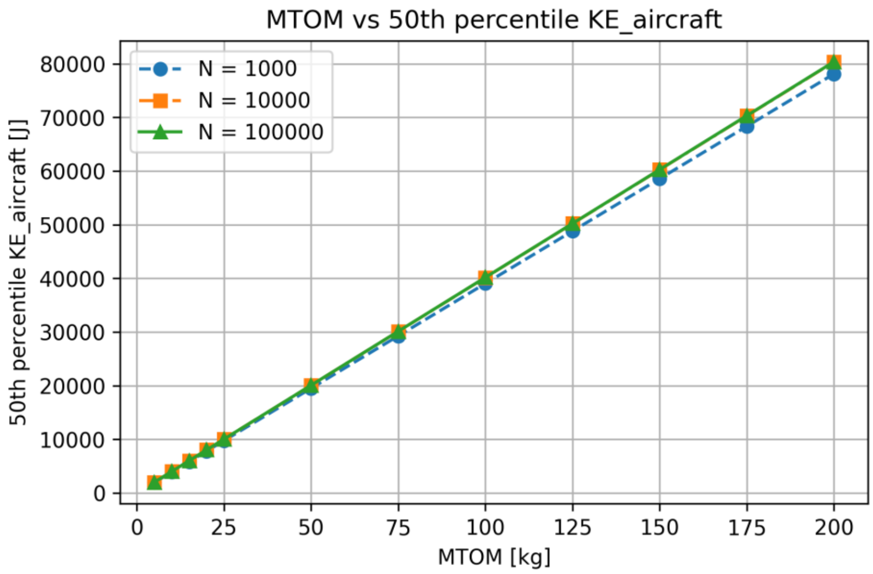

(a) The figure shows the median value of the estimated aircraft KE. A clear linear increase in the 50th-percentile aircraft KE with increasing aircraft mass can be observed.

Co-funded by the European Union

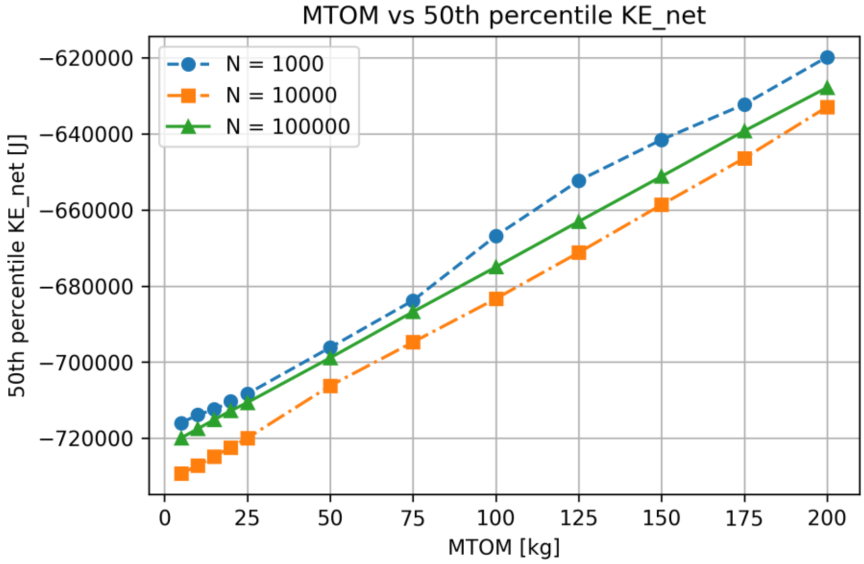

(b) This figure shows the median value of the difference between the aircraft kinetic energy (KE) and the maximum energy absorbable by the building. A clear linear trend of the KE difference with respect to MTOM can also be observed. The median (50th-percentile) value remains consistently negative over the entire MTOM range—ranging approximately from −720 kJ to −620 kJ—which is consistent with the fact that, in the majority of simulated cases, building penetration does not occur.

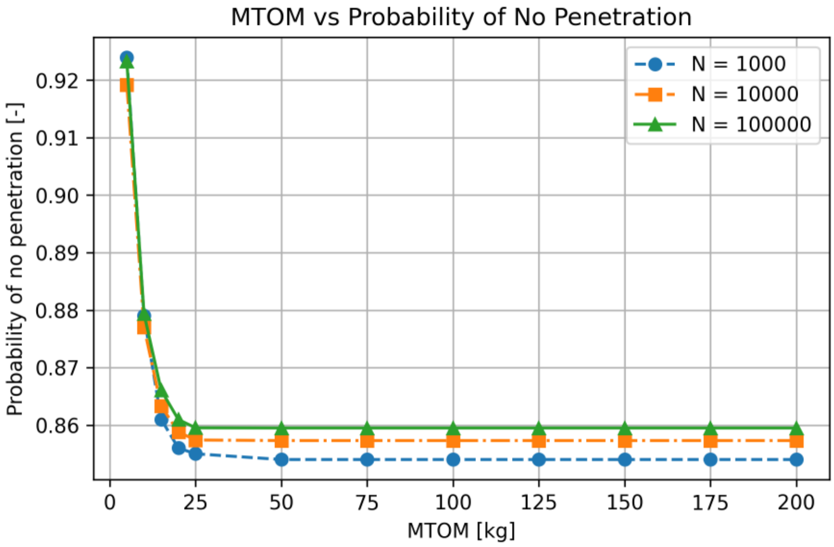

(c) This graph shows the probability of not penetrating a building versus the aircraft MTOM, one could observe that, for smaller aircraft (5 kg MTOM), we start from a probability of no penetration of approx. 92%, which drops significantly until a plateau is reached around 25 kg. After this limit, the probability of no penetration remains around 86%. This result indicates us that the probability of non-penetration is driven by the most fragile element (namely, the glass from which the windows are made).

Figure 3 - plots of results obtained for Case Study 2

3.1.3.3 Case study 3 – "mixed" fleet:

In Case Study 3, the sheltering response associated with a mixed fleet composition comprising 85% multirotor aircraft and 15% fixed-wing aircraft is assessed. For the purposes of the analysis, a material mix considered representative of a typical Italian multi-family residential building has been adopted (see Section 3.1.2.5 for further details).
The assumed distribution of building elements and the corresponding representative materials used in the analysis are summarised in Table 15: material mix for Case study 3

Building element	Representative material for penetration analysis	Percentage % (considering an average impact angle of 54.4 deg)
Roof	Reinforced concrete 100 mm - roof	32
Wall	Unreinforced Brick - wall	57
Windows	Gypsum/ fiberboard/ steel joist – roof (as derived from Table 7: UK Scenario, Window glazing/ glass may be assimilated to gypsum or lower for representativeness)	11

Table 15: material mix for Case study 3

Monte Carlo simulations were performed using $N = [1000,\ 10000, 100000]$ trials. The analysis covered a range of maximum take-off mass (MTOM) values, namely MTOM = [5, 10, 15, 20, 25, 50, 75, 100, 125, 150, 175, 200] kg.

The resulting median (50th percentile) values of:

- aircraft kinetic energy versus MTOM,
- net kinetic energy versus MTOM, and
- probability of penetration versus MTOM

are presented in **Error! Reference source not found.** (a), (b), and (c), respectively. A complete set of simulation outputs is provided in Appendix 0 for reference.

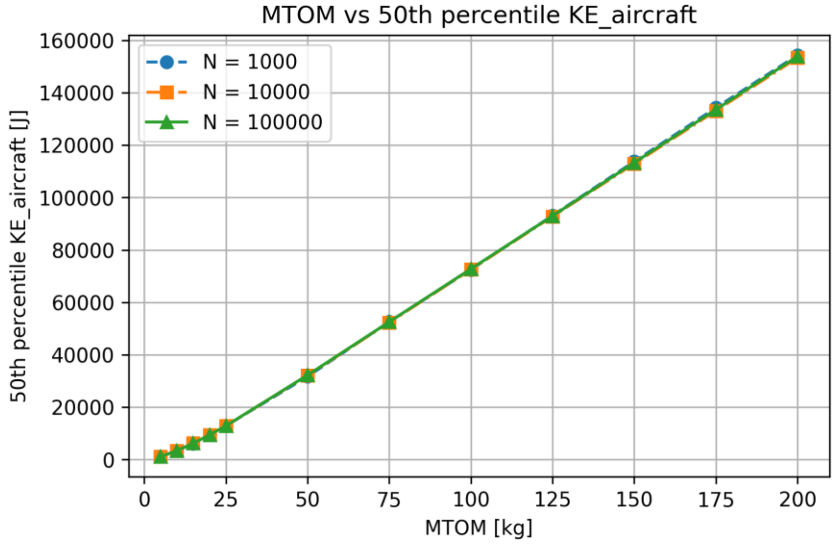

(a) The figure shows the median value of the estimated aircraft KE. A clear linear increase in the 50th-percentile aircraft KE with increasing aircraft mass can be observed.

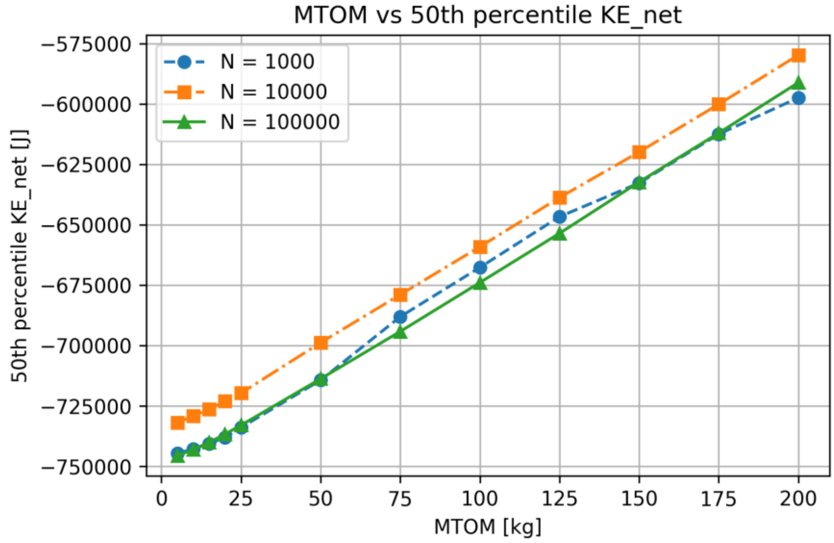

(b) This figure shows the median value of the difference between the aircraft kinetic energy (KE) and the maximum energy absorbable by the building. A clear linear trend of the KE difference with respect to MTOM can also be observed. The median (50th-percentile) value remains consistently negative over the entire MTOM range—ranging approximately from −750 kJ to −600 kJ—which is consistent with the fact that, in the majority of simulated cases, building penetration does not occur.

Co-funded by the European Union

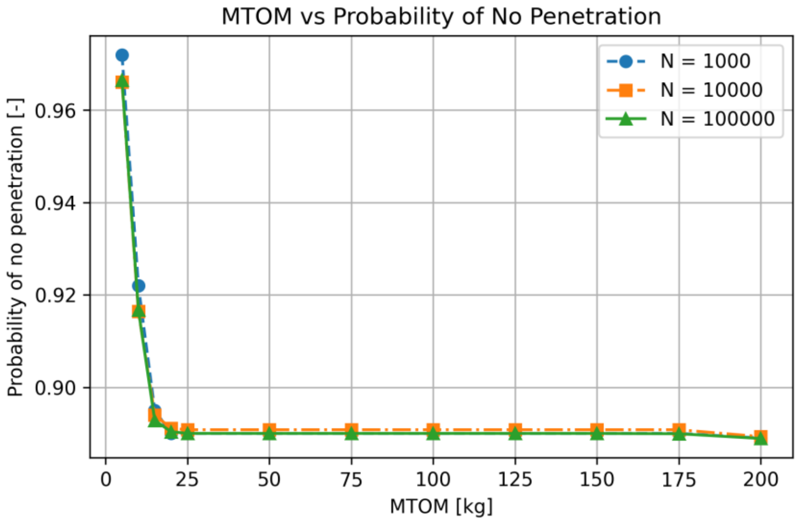

(c) This graph shows the probability of not penetrating a building versus the aircraft MTOM, one could observe that, for smaller aircraft (5 kg MTOM), we start from a probability of no penetration of approx. 97%, which drops significantly until a plateau is reached around 25 kg. After this limit, the probability of no penetration remains around 89%. This result indicates us that the probability of non penetration is driven by the most fragile element (namely, the glass from which the windows are made).

Figure 4 - plots of results obtained for Case Study 3

3.1.4 Conclusions

The model developed within the scope of this project introduces several substantial enhancements compared to the approach presented in [1]. In particular, it proposes an initial distinction between the impact dynamics of multirotor and fixed-wing UAS when assessing sheltering effectiveness, and explicitly accounts for both the building material mix and the probability of striking different architectural elements.

At a minimum, the model could be further refined through the following enhancements:

- by assigning different frontal area ranges as a function of the UAS MTOM category considered in the simulations. This refinement would be facilitated by the availability of a more comprehensive reference database than that available to the authors of the original study;
- by extending the simulation framework to account, for each Monte Carlo trial, for variations in the material mix as a function of the exposed surface areas (in square metres) of roofs, walls, and windows, and of the impact angle associated with each individual impact event;
- by explicitly modelling UAS equipped with parachute recovery systems (PRS) to reflect realistic operational constraints for large UAS (>25 kg) in urban and peri-urban environments where achieving operations in the Specific Category with low SAIL levels may be challenging without the use of a parachute.

The results obtained indicate that the probability of building penetration is largely dominated by the most fragile material present in the material mix—namely, window glazing in the present analysis. As a consequence, the non-penetration probability rapidly converges towards the percentage of glazing assumed in the simulation, already at MTOM values of approximately 25 kg, and subsequently decreases only marginally.

Fixed-wing aircraft exhibit a higher likelihood of entering a building through a window, primarily due to their characteristic impact dynamics. Conversely, materials typically used for roofs and walls in peri-urban and urban buildings in Italy are unlikely to be penetrated by UAS with MTOM below 200 kg.

It is important to note that the probability of striking a window has been evaluated assuming a single, isolated building. Future work could investigate how the effective material mix varies as a function of building density within a given area. In denser urban environments, where multiple buildings are present, the probability of a UAS impacting a window is expected to be lower than in the isolated-building scenario considered here.

Overall, these results suggest that, for Italian residential building typologies and for UAS with MTOM up to 200 kg, the supporting evidence required for the application of SORA M1(A) sheltering mitigation could primarily focus on a robust and justified estimate of the window percentage within the assumed material mix, as this parameter represents the dominant driver of building penetration likelihood.

3.2 Obstacle effect

3.2.1 Literature review

As discussed in [2], the assessment of obstacle effects can be also considered to obtain a reduction in iGRC for UAS missions conducted in urban environments. According to SORA 2.5 annex F [5], the methodology presumes that an aircraft will impact an area free of obstructions. This assumption is generally valid only for scenarios with very low iGRC levels (I-II). In urban contexts, however, the existence of obstacles such as buildings, trees, vehicles, and other structures means this assumption may not hold true. Accordingly, a comprehensive analysis of the obstacle environment can provide justification for reducing the assessed iGRC.

Indeed, from section 1.3 [5], iGRC can be expressed as:

$$\mathrm{iGRC} = \max\left(1, \left[7 + \log_{10}\left(D_{pop} A_c\right) - 0.5\right]\right)$$

Where:

- D_{pop} is the assumed maximum population density;
- A_c is the critical area;

It is possible to see that considering obstacles can directly impact the iGRC value through a reduction in the UAS average critical area. An example is provided below (figure 5).

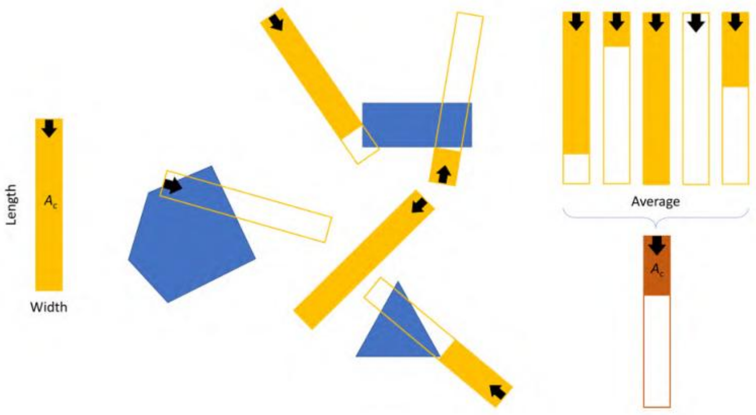

Figure 5 - How building presence can reduce the average critical area of multiple random crash. Source [5]

A reduction in the critical area can be seen as an M2 mitigation, reducing the effect of ground impact. As well as in Section 3.1, a Monte Carlo simulation with hundreds of random impact scenarios can be employed to estimate the critical area reduction resulting from obstacle presence. If this reduction exceeds 90%, then a reduction of one order of magnitude and an iGRC reduction of one level may be considered acceptable.

In the subsequent section, the SORA 2.5 Annex F simulation methodology will be formulated and implemented within multiple case studies to assess its potential as a mitigation strategy, identifying its applicability and limitations.

3.2.2 Implementation

Section B.4 of [5] addresses the role of obstacles in the ground risk model and their influence on UAS crash dynamics. Obstacles are represented as simplified physical entities whose primary function is to interact and stop an UAS in its post–loss-of-control trajectory. Rather than being modelled with full structural fidelity, obstacles are abstracted as geometric volumes (2D convex polygon) characterised by location, vertical extent, and interception capability.

To model this scenario, the following assumptions are made:

- The obstacles are considered sufficiently sturdy to stop the aircraft. In the majority of urban scenarios, it is reasonable to assume that an aircraft would impact the roof of a building; therefore, this assumption can be regarded as acceptable.
- The projection of the obstacles onto the ground can be represented well by a convex polygon. Specifically, obstacles are modeled as rectangles with characteristics dimensions ranging randomly (normal distribution) for each simulation in a specific interval.
- The x-y dimensions and location of the obstacles follow a normal distribution. This can lead to overlapping obstacles, but can be proved (as made in [5]) that this is a conservative hypothesis.
- Each drone fall is simulated, assuming the same critical area, by generating a random failure point within a 1 km² area, while the fall direction is also randomly assigned.

The implementation of this methodology can be divided into the following 4 steps:

1. Definition of the input;
2. Critical area estimation;
3. Urban scenario generation;
4. Multiple crash dynamic simulation with Monte Carlo loop and results extraction;

3.2.2.1 Input definition

The definition of input parameters plays a pivotal role in shaping the outcomes of both **critical area** calculation and **urban scenario** generation. Accurate and realistic inputs—such as obstacle dimensions, spatial distribution, and material properties—directly affect the estimation of the area at risk and the fidelity of the simulated urban environment. By carefully selecting and justifying these inputs, the methodology ensures that subsequent analyses reflect plausible real-world conditions, thereby enhancing the reliability and applicability of the results for risk assessment and operational planning.

The primary input definitions for critical areas focus on the physical attributes of UAS and their flight dynamic parameters. The mathematical model underlying the critical area is particularly significant. For this scenario, the approach (i.e. the mathematical model) described in deliverable 3.2 [2](Section 4.2), as detailed by JARUS in annex F section B.2, is used (figure 6).

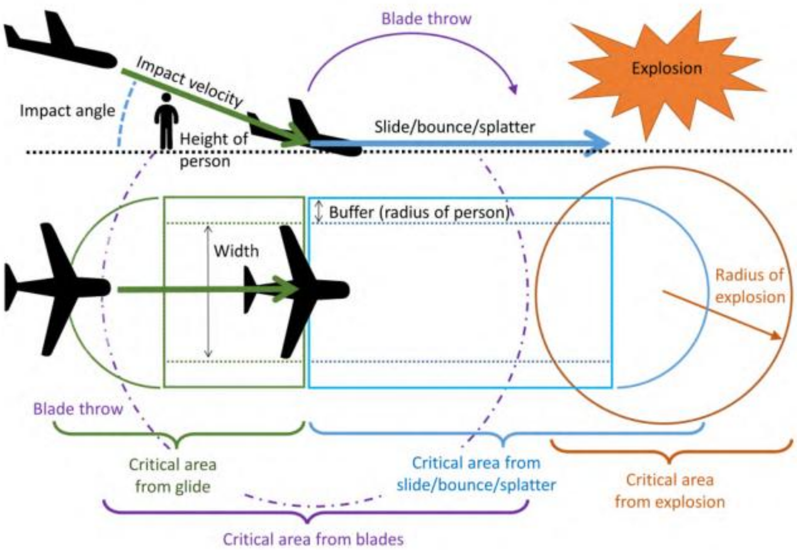

Figure 6 - Critical area modelling [5]

For buildings, instead, the modelling parameters regard their number, dimension and spatial distribution. Below follows table 16 explaining the input parameter that can be changed to influence the outcome of the simulations.

Critical Area estimation input	
MTOM [kg]	The Maximum Take Off Mass

V [m/s]	Impact speed – the magnitude of the speed vector
θ [deg]	Impact angle
μ [none]	Friction coefficient
$h_{obstacles}$[3]	Obstacles height
Urban scenario characteristics	
$D_{obstacles}$ [buildings/km^2]	Obstacles density
σ_x [m]	Buildings horizontal length standard deviation
μ_x [m]	Buildings medium horizontal length
σ_y [m]	Buildings vertical length standard deviation
μ_y [m]	Buildings medium vertical length

Table 16: Variable simulation inputs.

3.2.2.2 Critical Area estimation and urban scenario generation

To represent realistic operational scenarios while maintaining consistency across simulations, the following assumptions have been adopted:

- MTOM = 100 kg
  A sensitivity analysis was conducted by varying MTOM between 20 kg and 100 kg. Results show that, above approximately 100 kg, further increases in mass do not significantly affect the critical area. This is due to the fact that, beyond this threshold, the kinetic-energy-based lethality assumption dominates the calculation. For this reason, an MTOM of 100 kg is

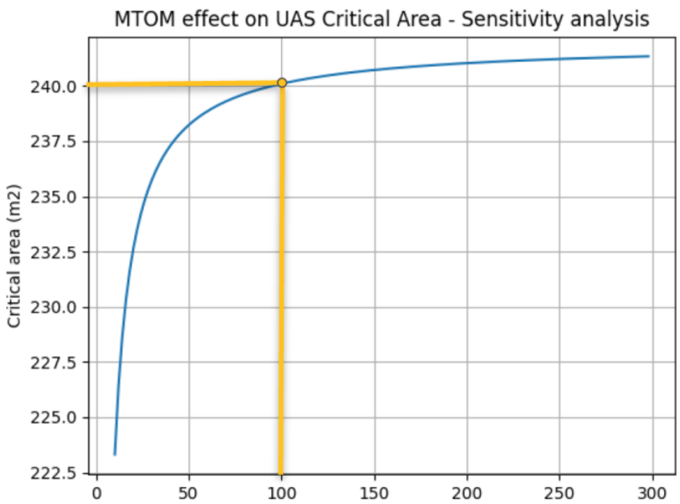

Figure 7 - MTOM sensitivity analysis on critical area

[3] The obstacles height is considered a parameter of the critical area and not of the urban scenario since it is used to directly estimate the critical area.

EUROPEAN PARTNERSHIP
Co-funded by the European Union

considered both representative of real operational cases and sufficient to capture MTOM effects in the model.

- Impact Speed:

  After a careful real Italian-use case scenarios[4] review, 2 different use case scenarios are considered during the simulations, in order to include both fixed-wing and rotorcraft missions:

  - For fixed-wing UAS, the impact speed value considered is: 30 m/s (with a CD = 4 m);
  - For rotorcraft UAS, the impact speed value considered is: 15 m/s (with a CD = 2 m);

- Impact angle :
  - 30° degree for the Fixed-wing UAS use case;
  - 50° degree for the rotorcraft UAS use case;
- Friction coefficient = 0.65

  Evidence [5] shows that this value ranges from 0.15 to 0.8. According to JARUS annex F section A 3.4, a conservative value of 0.65 has been chosen.

- The obstacles are as high as a medium Italian building (assumed 10 meters)[5];

Using these parameters, the resulting nominal critical areas are:

- Critical Area for fixed-wing UAS use-case = 207 m^2
- Critical Area for rotorcraft UAS use-case = 31 m^2

3.2.2.3 Urban environment definition

The parameters required to model the urban environment are those defined in Table 16.

For consistency with SORA v2.5, the definition of urban environments is grounded in the population-density bands defined in Annex F, which categorise areas as lightly populated, suburban/residential, or high-density metropolitan.

Density population range	Qualitative Descriptors

[4] ENAC approved operation list

[5] Residential building heights in Italy typically range from a few meters (with a minimum of approximately 2.7 m) up to about 15–20 m, excluding high-rise buildings. On this basis, a representative average obstacle height of 10 m has been assumed in the present analysis. In the original JARUS studies, buildings are conservatively modelled with a height equivalent to that of a standing person (1.8 m). For the purposes of this work, it was considered acceptable to relax this conservative assumption in order to better reflect realistic environmental conditions.

Co-funded by the European Union

$50\ ppl/km^2 < D_{pop} < 500\ ppl/km^2$	Suburban/Residential lightly populated
$500\ ppl/km^2 < D_{pop} < 5.000\ ppl/km^2$	Low density metropolitan
$5.000\ ppl/km^2 < D_{pop} < 50.000\ ppl/km^2$	High density metropolitan

Table 17: SORA 2.5 density bands

Specifically for the first parameter (population density), it is complex to define a single value in terms of building density in urban contexts, whether considering a single use-case municipality or using a more statistical approach on a national basis. For this reason, it has been necessary to make some assumptions. The 2025 EUROSTAT housing dataset [27], estimates an average of 2,3 persons per household.

With respect to the obstacle density parameter, there is currently no official indicator for building density in specific areas, as statistical agencies have not published explicit relevant data regarding this parameter. Nonetheless, the more generalist methodology proposed below, can be adopted in this study, with subsequent customization for distinct use cases when required.

Starting from population density, which can be estimated using different available dataset, the number of residential buildings per square kilometre can be derived through a structured conversion process that reflects how people are distributed within the built environment. Population density (expressed in inhabitants per km²) does not directly translate into a building density, as inhabitants occupy dwellings, and dwellings are in turn contained within residential buildings.

For this reason, the estimation requires the definition of two intermediate parameters: the average number of inhabitants per dwelling and the average number of dwellings per residential building. Based on the Eurostat Housing in Europe analysis [27], the number of inhabitants for dwelling can be assessed for individual countries (the average European value is 2,3 inhabitants per dwellings). Then, a different value of dwelling per residential building could be estimated based on the specific area considered. For example:

- In **lightly populated areas,** is common to find 1 to 2 family/dwellings per building;
- In **Suburban/Residential lightly populated area,** the number of dwellings per building typically ranges between 3 and 10;
- In **high-density metropolitan areas**, buildings often contain 10 or more dwellings.

The general relationship between these parameters can therefore be expressed as the ratio between population density and the product of these two intermediate parameters.

$$D_{obstacles} = \frac{D_{pop}}{N_{pd} \cdot N_{db}}$$

Where:

- $N_{pd} = Number\ of\ person\ per\ dwellings$
- $N_{db} = Number\ of\ \ dwellings\ per\ building$

This formulation makes all assumptions explicit, preserves dimensional consistency, and ensures that the resulting building density reflects the underlying settlement structure rather than relying on a direct but unsupported correlation between population and buildings.

Using this methodology, three use-case scenarios are studied:

- A **lightly populated area,** with a D_{pop} of $300\ ppl/km^2$ and 1 dwelling per building;
- A **Suburban/Residential lightly populated area,** with a D_{pop} of $3.000\ ppl/km^2$ and 5 dwellings per building;
- A **high-density metropolitan** area, with a D_{pop} of $30.000\ ppl/km^2$ and 10 dwellings per building.

Assuming an average of 2,3 persons per dwelling, we obtain the following obstacle densities:

$$D_{obs_1} = \frac{300\ ppl/km^2}{2{,}3\dfrac{ppl}{dwelling} \cdot 1\dfrac{dwelling}{building}} \approx 130\frac{building}{km^2}$$

$$D_{obs_2} = \frac{3000\ ppl/km^2}{2{,}3\dfrac{ppl}{dwelling} \cdot 5\dfrac{dwelling}{building}} \approx 261\frac{building}{km^2}$$

$$D_{obs_3} = \frac{30000\ ppl/km^2}{2{,}3\dfrac{ppl}{dwelling} \cdot 10\dfrac{dwelling}{building}} \approx 1304\frac{building}{km^2}$$

These values illustrate potential use-case scenarios; however, only use-cases 2 and 3 will be implemented, as they pertain to areas with greater building density where this methodology is most applicable.

Regarding the x-y dimension of the buildings ($\sigma_x, \sigma_y, \mu_x, \mu_y$), the same assumptions used by JARUS in section B.4 are made.

3.2.2.4 Monte Carlo Methodology and Convergence Analysis

The estimation of the critical area reduction factor due to the presence of obstacles in the urban environment is carried out through a Monte Carlo simulation approach. Since the interaction between the drone's critical area and the surrounding buildings depends on multiple stochastic variables — namely the impact position, the flight heading at the moment of failure, and the geometric variability of the obstacles — an analytical closed-form solution is not feasible. The Monte Carlo method provides a robust numerical framework to estimate the expected value of the reduction factor by repeatedly sampling these random variables and computing the resulting critical area reduction for each simulated impact.

For each iteration of the simulation, a random impact point is generated with uniform distribution over the analysis area (1 square kilometre), and a random heading angle is sampled uniformly between 0° and 360°. The oriented critical area footprint is then constructed at the sampled location and direction, and its geometric intersection with the obstacle field is evaluated. The output of each individual simulation is the residual critical area expressed as a percentage of the original, unreduced critical area. The overall result of the Monte Carlo analysis is the average of this quantity across all simulated impacts, representing the average fraction of critical area that remains exposed after accounting for obstacle sheltering.

A key requirement for any Monte Carlo analysis is to demonstrate that a sufficient number of iterations have been performed for the result to be statistically stable. To this end, a formal convergence criterion has been adopted. Rather than fixing an arbitrary number of simulations, the analysis proceeds incrementally in blocks of fixed size and evaluates the stabilisation of the cumulative mean after each block. Specifically, the relative deviation between the cumulative mean at iteration N and the cumulative mean at the previous evaluation point N−k is computed as:

$$\Delta = \frac{|\mu_N - \mu_{N-k}|}{\mu_N}$$

Where:

- Δ is the relative deviation for each step of the simulation;
- μ_i is the cumulative mean at step i;
- k is the step size.

Convergence is declared when this relative deviation remains below a predefined threshold for a specified number of consecutive blocks, ensuring that the result is not affected by transient fluctuations.

The convergence parameters adopted for the present analysis are summarised as follows:

- a step size of 500 simulated impacts;
- a relative deviation threshold of 1%;
- and a requirement of 10 consecutive blocks below threshold before convergence is declared.

These parameters have been selected to balance computational efficiency with the need for a reliable and repeatable estimate of the critical area reduction factor. Results are presented in the following section.

3.2.3 Obstacles simulation results

The results obtained with the methodology and use cases presented in section 3.2.2 are here examinated.

3.2.3.1 Fixed-wing analysis

As can be seen in Figures 8-9, the reduction of critical area achieved by considering the sheltering effect related to the presence of buildings in the case of fixed-wing aircraft is:

- A reduction of approximately 18.5% in suburban environments (residual critical area 81.5%);
- A reduction of about 61% in metropolitan environments (residual critical area 39%).

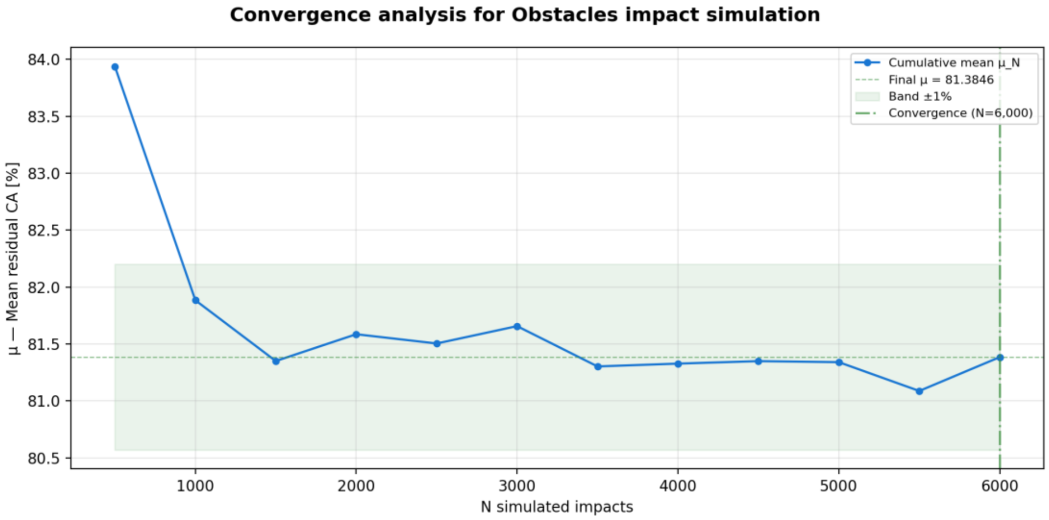

Figure 8 - Convergence analysis for Fixed-wing in use-case 1 scenario (Suburban).

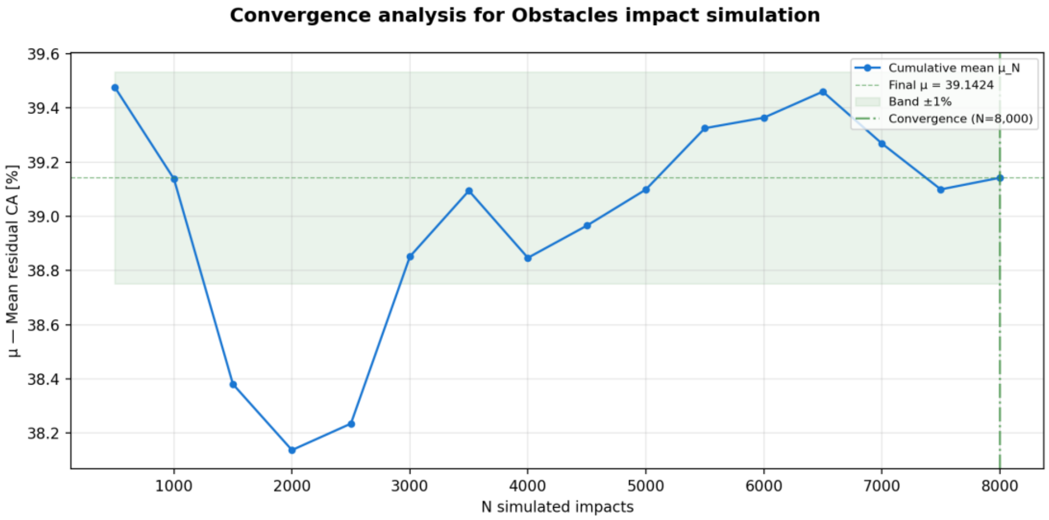

Figure 9 – Convergence analysis for Fixed-wing in use-case 2 scenario (High-density metropolitan areas).

3.2.3.2 Rotorcraft analysis

Figures 10 and 11 show the results obtained in use-case 1 and 2 considering instead a rotorcraft UAS. As predictable, dealing with a lower critical area, the obstacles effect is less impactive, resulting in:

- A critical area reduction of 9% from its nominal value (91% of mean residual CA);
- A critical area reduction of 37% from its nominal value (63% of mean residual CA);

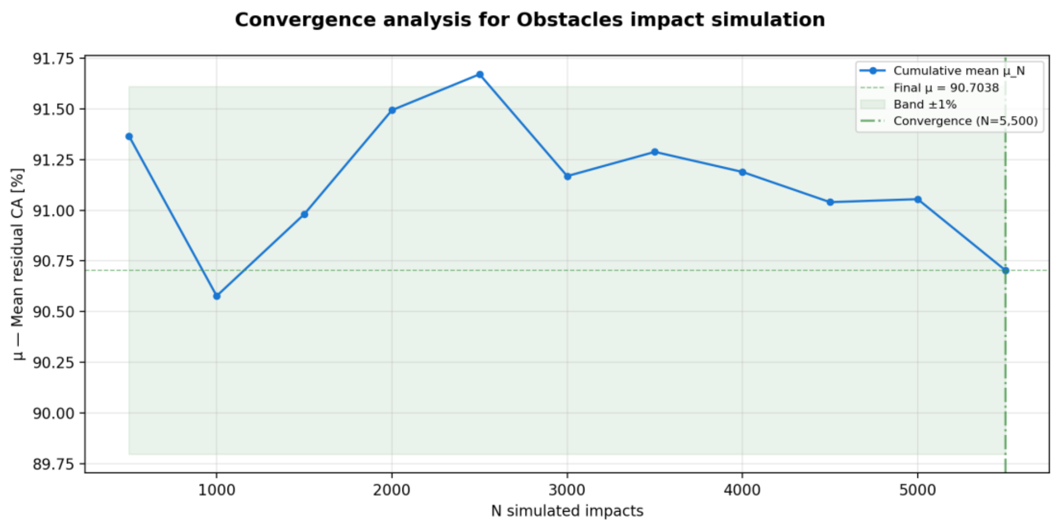

Figure 10 - Convergence analysis for rotorcraft in use-case 1 scenario (Suburban).

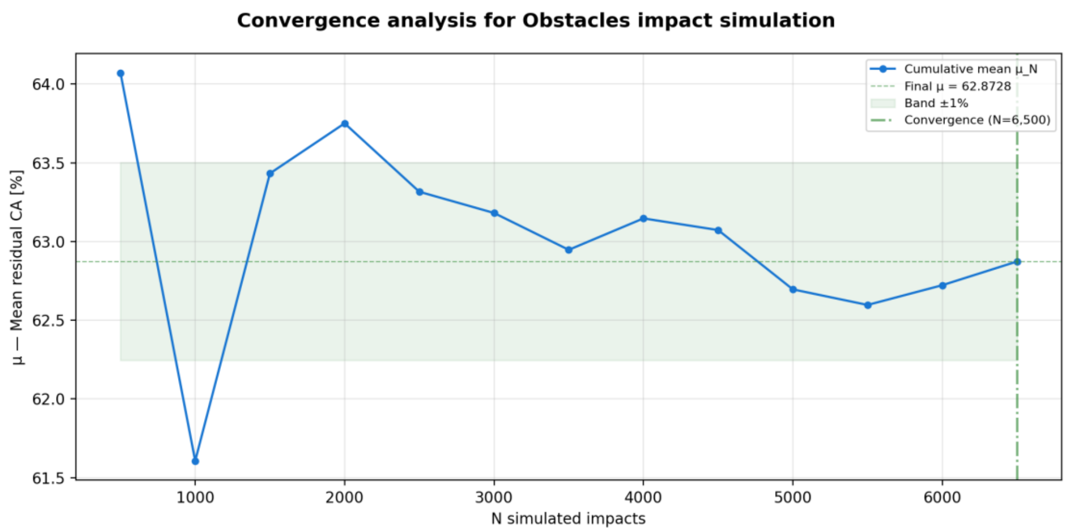

Figure 11 - Convergence analysis for rotorcraft in use-case 2 scenario (High-density metropolitan areas).

3.2.4 Findings and conclusion

The study of the sheltering effect due to the presence of urban buildings has highlighted both the strengths and the limitations of this potential mitigation approach within the SORA framework. Regarding the suburban scenario, although these environments already pose significant challenges when conducting a SORA analysis — typically requiring the implementation of substantial mitigation measures — the results obtained show that the building density characteristic of suburban areas is still insufficient to achieve a meaningful reduction of the critical area through obstacle sheltering alone.

The situation changes significantly in metropolitan and high-density urban areas. For both UAS typologies, a considerably higher critical area reduction was observed. Specifically, Fixed-wing UAS achieved a reduction exceeding 60%, while rotorcraft yielded a reduction slightly below 40%. Although neither value is sufficient on its own to achieve a reduction in the iGRC — which, according to the Annex F framework, would require a sheltering factor in the order of 90% — these results are nonetheless significant. They suggest that obstacle sheltering could be introduced as a complementary mitigation measure in cases where other mitigation strategies alone are unable to reach the threshold required for an iGRC reduction.

The analysis has highlighted the differences in the applicability of this approach between fixed-wing and rotorcraft configurations, showing a greater potential for sheltering-based mitigation in the fixed-wing case due to the larger and more elongated critical area footprint.

The work presented here constitutes an initial contribution that could be further generalised, refined — for relaxing other conservative hypothesis, such as the random distribution of buildings — and supported with more accurate data, with the goal of being fully integrated into Step #3 of the SORA process as a recognised supplementary mitigation measure in complex urban scenario operation.

3.3 Extended Assessment of the Severity of Negative Effects from UAS Ground Impacts and from UAS Operations

Drone operations can result in a range of negative effects beyond direct safety risks. This section builds on the SORA Ground Risk Model, and in particular on the latest version of SORA Annex F, by providing a structured framework for UAS operators and competent authorities to better estimate the severity of such effects. In addition to injury-related consequences from direct ground impacts, the assessment explicitly considers environmental (e.g. noise and visual pollution), economic, and reputational effects, as well as impacts arising from other operational events. By enabling the qualitative and quantitative scoring and weighting of these factors based on expert judgement, this extended severity assessment enhances the completeness and robustness of the ground risk model. All assessments are intended to be performed at the planning stage, before operations take place, supporting more informed risk classification, mitigation selection, and integrated risk model development.

3.3.1 Domains of Negative Effects

3.3.1.1 Ground Impacts

Extending the analyses of the severity of a UAS crashing on the ground to include environmental aspects such as noise or visual pollution, as well as economic and reputational impacts, would require access to comprehensive historical UAS crash data. However, this is currently not feasible due to the limited availability of such data. The lack of documented incidents, especially with detailed post-crash impact assessments, hampers the ability to draw meaningful conclusions or establish robust risk models for these domains.

Ground impacts from UAS crashes can produce a spectrum of negative effects that extend well beyond immediate safety concerns. Recent incident analyses 73[8] show that such events frequently result in environmental disturbances (including noise, visual pollution, and hazardous material release), direct and indirect economic losses (such as property damage and service disruption), and significant reputational consequences for operators and the wider industry. These impacts are often compounded by equipment failures, adverse environmental conditions, and organisational or policy shortcomings.

Complementing this perspective, a study [9] highlights that, in addition to the risk of fatalities, UAS ground impacts can cause substantial property damage, environmental harm (such as fire or chemical spillage), and broader societal effects including public discomfort and loss of confidence, especially when incidents occur near sensitive locations or with high frequency. The cost of a UAS ground impact thus encompasses not only direct consequences for people but also property, the environment, and reputation.

The following list identifies broad domains in which negative effects from ground impacts may occur, as well as specific factors within each domain that can be used to assess and compare the severity of these impacts. The domains of negative effects related to ground impacts can include:

- Environmental:
  - Noise (e.g., acute and persistent exposure).
  - Visual pollution (e.g., debris, wreckage visibility).
  - Release of hazardous materials (e.g., battery chemicals, fuel, payload).
  - Local air pollution from combustion or material release.
  - Fire risk and secondary environmental damage.
  - Soil and water contamination at the crash site.
  - Impact on flora and fauna in the immediate area.
  - Etc.
- Economic:
  - Area or population affected by economic loss.
  - Estimated cost of property damage, service disruption, etc.
  - Etc.
- Reputational:
  - Public sentiment or acceptance following incidents.
  - Operator or industry reputation metrics.
  - Frequency and severity of incidents affecting public trust.
  - Etc.

3.3.1.2 Other-than-Ground Impacts

This section presents various performance indicators that can be assessed during typical UAS operations or other non-ground impact events. These indicators cover areas such as noise and visual pollution, privacy issues, emissions, effects on wildlife, economic factors, and security considerations.

The following list identifies broad domains in which negative effects from UAS operations may occur, as well as specific factors within each domain that can be used to assess and compare the severity of these operations. The domains of negative effects related to other-than-ground impacts can include [10]:

- Noise Pollution:
  - Number of people exposed to noise above a threshold.
  - Exposure to noise during day, evening, and night periods.
  - Exposure along drone trajectories.

  - Duration of exposure to elevated noise.
  - Difference between drone and background noise.
  - Intermittency of noise events.
  - Event frequency and population exposure.
  - Etc.
- Visual Pollution:
  - Number of people able to see a drone during operations.
  - Number of people exposed above a visual pollution concentration threshold.
  - Duration of visual exposure.
  - Area-based and trajectory-based exposure counts.
  - Visual exposure per kilometre travelled.
  - Etc.
- Privacy:
  - Survey-based perception of privacy intrusion.
  - Number of people exposed to potential surveillance.
  - Duration of time individuals are subject to observation.
  - Exposure to hovering drones at close range.
  - Etc.
- Emissions:
  - CO_2 emissions per flight.
  - Energy consumption for drone operations.
  - Area-based and trajectory-based emissions.
  - Etc.
- Wildlife:
  - Number of animals exposed to drone activity.
  - Annoyance or disturbance metrics for wildlife.
  - Changes in wildlife population or behaviour.
  - Exposure and annoyance levels for specific scenarios.
  - Etc.
- Economic:
  - Area of negative economic influence (e.g., job loss, property value change).
  - Etc.
- Security:
  - Frequency of unauthorised access or interference with drones (e.g., hacking, jamming, etc.).
  - Vulnerability scores for drone operations (e.g., susceptibility to cyber-attacks, etc.).
  - Incidents of data breach or loss of sensitive information.
  - Etc.

3.3.2 Severity Scores

3.3.2.1 Ground Impacts

3.3.2.1.1 Qualitative Assessment

The severity score structure outlined below enables drone operators to classify the severity of negative effects associated with drone crashes in a qualitative manner. Each effect is assigned a severity score (High (2), Medium (1), or Low (0)) based on its severity across several domains listed in 3.3.1.1.

It is important to note that, within this assessment, the economic impact considered does not include the financial loss to the drone operator resulting from the destruction or loss of the drone itself. Similarly, environmental and reputational impacts are assessed solely in terms of their effects on external parties, environments, or organisations, and do not account for consequences experienced internally by the operator.

Level	Score	Environmental	Economic	Reputational
High	2	Crash in highly sensitive area (e.g., national park, urban centre, wildlife zone, etc.); severe noise, visual, or chemical pollution, many people or sensitive environments affected.	Significant financial damage; crash causes major disruption to infrastructure, services, or property (e.g., road closure, service interruption, etc.).	Viral or international media coverage; long-term trust damage, regulatory scrutiny, widespread public awareness.
Medium	1	Crash near a park, school, or environmentally protected zone, etc.; noticeable pollution, moderate exposure.	Minor damage to private property or public infrastructure; minor disruption or repair costs.	Local or regional media coverage; temporary stakeholder concern, minor complaints.
Low	0	Crash in remote or industrial area; minimal pollution, few or no people affected.	No financial damage; crash on empty land, no third-party damage or service disruption.	No media attention, no public awareness; incident handled internally, no escalation.

Table 18: Severity score for negative effects related to ground impacts.

3.3.2.1.2 Quantitative Assessment

It should be noted that the available quantitative data drawn from existing research is limited, and as such, the precision of severity assessments may be constrained. However, to support operators and facilitate future research, guidance and methodologies adapted from alternative sectors is also provided in this section, enabling the quantification or extension of these assessments as more data becomes available.

3.3.2.1.2.1 Environmental Impact

To assess the potential environmental severity impact of a drone crash, operators can treat the event as an impulse noise similar to that produced by heavy impact equipment. The evaluation could follow a structured process to estimate the severity of noise effects relative to the surrounding environment [11].

To systematically assess the environmental noise impact of a drone crash, an estimation can be done of the peak noise level generated by the drone upon impact. This can be done by referencing available data from similar impact events or, if such data is unavailable, by using analogies to known sources such as jackhammers or pile drivers. The aim is to establish a realistic starting point for the noise level that would be produced during a crash.

Common Sounds	Noise Level (dB)	Effect
Rocket launching pad (no ear protection)	180	Irreversible hearing loss
Carrier deck jet operation Air raid siren	140	Painfully loud
Thunderclap	130	Painfully loud
Jet takeoff (200 feet) Auto horn (3 feet)	120	Maximum vocal effort
Pile driver Rock concert	110	Extremely loud
Garbage truck Firecrackers	100	Very loud
Heavy truck (50 feet) City traffic	90	Very annoying Hearing damage (8 hours)
Alarm clock (2 feet) Hair dryer	80	Annoying
Noisy restaurant Freeway traffic Business office	70	Telephone use difficult
Air conditioning unit Conversational speech	60	Intrusive
Light auto traffic (100 feet)	50	Quiet
Living room Bedroom Quiet office	40	Quiet
Library/soft whisper (15 feet)	30	Very quiet
Broadcasting studio	20	Very quiet
	10	Just audible
Threshold of hearing	0	Hearing begins

Figure 12 - Sound levels and human response [11].

Equipment	dBA	Equipment	dBA
Heavy trucks (avg.)	82–96	Backhoe (avg.)	72–90
Grader (avg.)	79–93	Paver (+ grind) (avg.)	85–89
Excavator (avg.)	81–97	Front loader (avg.)	72–90
Crane (avg.)	74–89	Generator (avg.)	71–82
Pile driver (peak)	81–115	Jackhammers/rock drills (avg.)	75–99
Concrete mixer (avg.)	75–88	Roller (avg.)	72–75
Compressor (avg.)	73–88	Pumps (avg.)	68–80

Figure 13 - Noise ranges at 15 meters from common construction equipment [11].

Next, operators can determine the baseline or ambient noise level at the operational site. This involves either measuring the typical background noise using a sound level meter or consulting published values for similar environments, such as urban, suburban, or rural areas. Establishing the ambient noise level is crucial, as it serves as the reference against which the significance of the drone impact noise will be assessed.

The third step is to characterise the site conditions where the crash may occur. Operators can identify whether the surface is hard (such as concrete, asphalt, water, etc.) or soft (such as grass, soil, etc.).

Co-funded by the European Union

This distinction is important because hard surfaces reflect sound, resulting in less attenuation, while soft surfaces absorb sound, leading to greater attenuation as the noise travels away from the source.

Following this, the operator can classify the nature of the noise source. In most cases, a drone crash will be treated as a point source, a single, localised event. However, if the crash results in debris or secondary impacts over a wider area, it may be appropriate to consider a line source model, which has different attenuation characteristics.

With these factors established, the operator can model how the noise level decreases with distance from the impact site. Standard attenuation rates are applied: for point sources, the noise typically decreases by a set amount for each doubling of distance, with the rate depending on whether the site is hard or soft. Additional factors such as vegetation, topography, and atmospheric conditions can further reduce noise, though these are often difficult to quantify precisely and may be considered as qualitative modifiers.

The operator then compares the estimated noise levels at various distances to the ambient noise level. The distance at which the impact noise becomes indistinguishable from the background noise defines the “zone of noise impact”, the area where the environmental effect is considered significant. This process can be documented in a table or graph, showing the relationship between distance and noise level. Additionally, it would be advantageous to implement a shared database that operators can populate as crashes occur or as further testing is conducted. Over time, such a database would accumulate valuable real-world data on crash conditions, noise levels, and environmental characteristics. Ideally, an operator can then utilise this resource to identify scenarios that closely match their own operational conditions and, through the use of generalised calculation factors, automatically obtain the “zone of noise impact” relevant to their situation.

For sensitive environments, such as those near wildlife habitats, operators can also consider species-specific hearing thresholds and potential behavioural or physiological effects.

3.3.2.1.2.2 Economic Impact

The economic impact of UAS ground impacts is multifaceted, encompassing direct costs such as property damage, vehicle collisions, and potential harm to critical infrastructure, as well as indirect costs related to public perception, regulatory changes, and insurance requirements. Analyses of military and civil drone accidents reveal that high-severity incidents (Class A and B) are associated with substantial economic consequences. In the reviewed dataset, Class A accidents, defined as crashes leading to complete destruction of the UAV and approximately USD 2 million in damage, account for 192 recorded incidents, while Class B accidents, involving complete or partial UAV destruction with damages between USD 2 million and USD 5 million, account for 224 incidents. For example, within the U.S. Air Force Predator fleet, approximately 40 % of acquired aircraft were lost in Class A accidents and a further 8 % in Class B accidents, highlighting the prevalence of these high-severity outcomes [12]. Furthermore, the probability of such impacts is influenced by factors including UAS reliability, operational environment, and population density, with risk models quantifying expected casualties and property losses per flight hour [13]. In urban settings, the risk of economic loss is heightened due to dense populations and valuable infrastructure, necessitating comprehensive severity assessment frameworks that account for collision probabilities, debris dispersion, and third-party liability [13]. The cumulative effect of frequent, even non-fatal, drone incidents can also drive-up insurance premiums, increase regulatory compliance costs, and erode public trust, all of which have significant economic implications for operators and society at large [12].

Recent mathematical modelling of the financial impact of air crashes [14] demonstrates that such incidents have an immediate and statistically significant negative effect on the stock prices and market value of the involved airlines, especially in fatal events. The effect is most pronounced on the day of the event and typically dissipates within a few days, but reputational damage and loss of consumer trust can have longer-term financial consequences. In contrast, manufacturers are less affected unless the crash is directly attributed to a manufacturing fault [14]. For listed companies, the short-term financial impact can be quantified using the abnormal return (AR) and cumulative abnormal return (CAR) formulas:

$$AR_{it} = R_{it} - E(R_{it})$$

$$CAR_{ie} = \sum_{t_1}^{t_2} AR_{it}$$

Where:

- AR_{it} = abnormal return for company $i$at time t
- R_{it} = actual return
- $E(R_{it})$= expected return (using a market model or Fama-French model)
- CAR_{ie} = cumulative abnormal return over the event window

While the above financial impact model is well established for listed companies, UAS operators are typically not publicly traded entities and therefore do not experience measurable stock-market reactions such as AR and CAR. Nevertheless, the underlying economic logic remains applicable. For UAS operators, the consequences of an accident are reflected through direct operational disruptions, loss of contracts, increased insurance premiums, regulatory scrutiny, reputational damage, and reduced customer trust, rather than immediate market valuation effects. As a result, although the same quantitative market-based indicators cannot be directly applied, the model provides a useful conceptual framework to understand how safety-critical events translate into short-, medium- and long-term financial impacts for UAS operators, with differences arising primarily from the nature and scale of their business structures.

Reputational damage can also increase a firm's credit risk. A study [15] demonstrates that after major aviation accidents, the probability of default (PD) for airlines rises significantly, as measured by the CreditGrades model:

$$\text{In} \left(\frac{PD_j}{PD_i} \right)$$

Where PD_j and PD_i are the probabilities of default after and before the crash, respectively. Empirical results show a mean PD increase of around 22% one week after a crash, with effects persisting for up to a year [15].

In other studies, as shown in [13] the cost of property damage (C_b) is modelled as a function of building height, with the risk cost increasing according to the log-normal distribution of building heights:

$$f(h,\mu,\sigma)=\frac{e^{-(\ln h-\mu)^2/2\sigma^2}}{h\sigma\sqrt{2\pi}}$$

The table below summarises the risk cost formula above based on building height:

Building Height (h)	Risk Cost Formula
$0 < h \leq e^{u}$	$C_b = f(e^{h})$
$h > e^{u}$	$C_b = f(h)$

Table 19: Relation between risk cost and building height [13].

Where h is the building height and u is the mean (location parameter) of the log-transformed building height distribution. This approach allows for a more accurate estimation of economic losses in urban environments, where building density and value are high.

Additionally, as illustrated in the image below real-world drone crash scenarios demonstrate the potential for significant property and infrastructure damage, reinforcing the need for robust economic severity assessment and mitigation strategies.

Figure 14 – Drone crash near a civil house in Seychelles [12].

3.3.2.1.2.3 Reputational Impact

Quantifying the reputational impact of UAS ground crashes requires a combination of qualitative and quantitative approaches, as recommended by [16] and supported by recent UAS incident research [7].

The reputational impact of drone ground crashes is profound, extending well beyond immediate environmental or financial impacts. Media coverage, stakeholder feedback, and social sentiment play a critical role in shaping public perception and trust in both the operator and the broader industry. Research on major aviation disasters, such as the Boeing 737-MAX incidents, demonstrates that negative media attention and stakeholder reactions can trigger a contagion effect, damaging not only the directly involved company's reputation but also that of other industry players [17].

As per [16], media analysis, web sentiment, and customer feedback are essential tools for monitoring and quantifying reputational risk. To quantify the reputational impact of a UAS ground crash, [16] applies the event study methodology, which measures the drop in a company's market value following the public announcement of the incident; specifically, it calculates AR and CAR over a defined event window, attributing any loss in market value that exceeds the direct operational costs to reputational damage. This approach, supported by empirical analysis of 37 international cases, demonstrates that reputational loss is statistically significant and often persists beyond the immediate aftermath, making CAR a robust quantitative indicator for reputational impact [16].

Incident analysis in the UAS sector highlights that reputational risks are amplified by gaps in safety culture, inadequate communication, and policy deficiencies [7].

3.3.2.2 Other-than-Ground Impacts

3.3.2.2.1 Qualitative Assessment

The severity score structure outlined below enables drone operators to classify the severity of negative effects associated with drone operations in a qualitative manner. Each effect is assigned a severity score (High (2), Medium (1), or Low (0)) based on its severity across several domains listed in 3.3.1.2.

It is important to clarify that, within the evaluation of the negative effects associated with other-than-ground impacts, the severity scores presented in the table below relate solely to external consequences. Specifically, the assessment excludes any internal impacts or losses sustained by the drone operator, such as operational disruptions or equipment damage. Instead, the focus is placed on the extent of adverse effects experienced by the wider community, environment, and public stakeholders, covering aspects such as noise and visual pollution, privacy breaches, emissions, wildlife disturbance, economic repercussions, and security risks.

Level	Score	Noise Pollution Impact	Visual Pollution Impact	Privacy Impact [13]	Emissions Impact	Wildlife Impact	Economic Impact	Security Impact
High	2	Drone operations cause severe noise disturbance; widespread annoyance or health risk in densely populated or sensitive areas.	Drone operations cause severe visual disturbance; large population exposed (e.g., urban centre, public events, etc.).	Drone operations in areas with strong privacy protection requirements (e.g., government institutions, sensitive venues, etc.).	Drone operations result in significant emissions (e.g., frequent fossil fuel use, regulatory limits exceeded, etc.).	Drone operations cause severe disturbance to wildlife, especially in protected or sensitive habitats.	Drone operations cause significant negative economic effects (e.g., job loss, reduced property values, business disruption, etc.).	Drone operations in populated areas or near critical infrastructure where unauthorised data interception can compromise public safety or national security or where GPS spoofing/jamming can cause severe consequences (e.g., collision risk, disruption of emergency services).
Medium	1	Noticeable noise disturbance; moderate annoyance or exposure in suburban or moderately populated areas.	Noticeable visual disturbance; moderate number of people exposed (e.g., suburban, small town, etc.).	Drone operations in areas with moderate privacy protection requirements (e.g., villa districts, private venues, etc.).	Some emissions released; near regulatory limits, minor environmental impact.	Noticeable wildlife disturbance; minor exposure in suburban parks or edge of habitat.	Some negative economic effects (e.g., minor changes in property value, small business impact, etc.).	Drone operations in suburban or moderately populated areas, where weak encryption or authentication can expose customer data during delivery missions or allow firmware tampering. Severity increases when drones operate

Level	Score	Noise Pollution Impact	Visual Pollution Impact	Privacy Impact [13]	Emissions Impact	Wildlife Impact	Economic Impact	Security Impact
								close to private properties or commercial venues.
Low	0	Negligible noise impact; few or no people exposed, rural or remote areas.	Negligible visual impact; few or no people exposed, rural or remote areas.	Drone operations in areas without privacy protection requirements (e.g., public spaces, etc.).	Negligible emissions; electric drones, below baseline or regulatory limits, no environmental impact.	Negligible wildlife impact; no wildlife exposed or disturbed, non-sensitive areas.	Negligible economic impact; no measurable effect on jobs, property values, or business.	Drone operations in remote or rural areas with robust security measures (e.g., encrypted communication, secure firmware, etc.), where the severity of malicious interference is low/none and no sensitive data is transmitted.

Table 20: Severity score for negative effects related to other-than-ground impacts.

3.3.2.2.2 Quantitative Assessment

It should be noted that, while quantitative data for noise and visual pollution is more prevalent due to extensive practical research in these domains [18], there remain certain limitations in the precision of severity assessment models. Nevertheless, to assist operators and encourage ongoing improvements, this section also offers guidance and methodologies adapted from related sectors, providing a framework for quantifying or refining assessments as additional data and insights become available.

3.3.2.2.2.1 Noise Pollution Impact

To quantify noise pollution from drone operations, [13] proposes a spatially explicit risk indicator model that divides the operational airspace into a three-dimensional grid. For each grid cell, the noise risk indicator is calculated as

$$R_n = \left(L_g - L_0 + \varphi\right)(1 - \tau E_n) A_n \rho_n$$

Where:

- R_n: Noise risk indicator for grid n.
- L_g: Instantaneous sound level of UAS noise reaching the ground; $L_g = L_s - \Delta L$.
- L_s: Sound level generated by the UAS as the sound source.
- L_0: Instantaneous sound level on the ground in the absence of UAS.
- φ: Correction factor.
- E_n: Barrier effect (sound barrier/exposure factor).
- A_n: Area of grid n.
- ρ_n: Population density within grid n.

Complementing this, [10] define seven quantitative noise pollution indicators (NO-1 to NO-7) focused on human exposure: NO-1 and NO-2 measure the number of people exposed to noise above a threshold (either over a fixed period or across day/evening/night); NO-3 and NO-4 assess exposure along drone trajectories and per noise event; NO-5 quantifies the duration of exposure; NO-6 captures the difference between drone and background noise; and NO-7 evaluates the proportion of intermittent to continuous noise. These indicators use units such as “person” or “dB·person” and are designed for practical application with real operational data, supporting comprehensive, people-centred quantification of UAS noise impacts.

Building on this framework, [11] demonstrate a practical methodology that integrates high-resolution drone trajectory modelling, advanced noise emission and propagation simulation, and dynamic population mapping using mobile network and GPS data. Key indicators such as NO-1 ($L_{A_{eq}}$), NO-2 (L_{DEN}), and NO-5 (exposure duration) are calculated by overlaying noise maps with temporally and spatially resolved population data, enabling segmentation by demographic factors such as age and gender. For example, in a Madrid case study, the NO-5 indicator revealed that the 25–44 and 45–64 age groups experienced the highest exposure during a cruise flight, while NO-1 showed that 9,430 people were exposed to noise above the threshold during a take-off event, with the impact concentrated near the flight path [18].

3.3.2.2.2.2 Visual Pollution Impact

Similarly, [10] defines a set of quantitative visual pollution indicators (VP-1 to VP-9) to capture the impact of drone operations on public perception and well-being: VP-1 and VP-2 measure the number of people exposed to drone visibility or to a visual pollution concentration above a threshold during a single operation; VP-3 and VP-4 extend this to exposure over a specified duration or quantify total visual exposure along a trajectory; VP-5 to VP-7 aggregate these metrics at the area level, considering the number of people exposed, the duration, and the concentration threshold; VP-8 calculates the total visual exposure perceived by all affected people in an area; and VP-9 expresses visual exposure per kilometre travelled, normalised by population density. These indicators use units such as “person”, “person·vp·h”, or “person/km”, and are designed for practical, high-resolution assessment of visual disturbance from UAS, supporting people-centred and context-sensitive management of urban drone operations.

Building on this, [18] presents a robust methodology for quantifying visual pollution that combines GIS-based landscape analysis with dynamic, high-resolution population mapping. Central to this approach is the visual pollution concentration (VPC) metric, which can be calculated using the AiRMOUR formula:

$$\text{VPC} = 47.76 \cdot \frac{N^{0.65}}{D^{0.67}} + 1.37$$

Where:

- N: Number of visible drones and D is the distance to the observer.

Alternately, it can be calculated by comparing the area occupied by the drone in the observer’s field of view to the open sky, which can be calculated using the following formula:

$$\text{VPC} = CF\frac{\sum_i^N \Omega(\text{drone}_i)}{\Omega(\text{open sky})} = CF\frac{\sum_i^N \text{atan}\left(\frac{a_i}{R_i^2}\right)}{4\pi - \Omega(urban)}$$

where:

- CF: Normalisation constant, $CF = \frac{2\pi}{atan\left(\frac{1}{100^2}\right)}$
- N: Number of drones visible to the observer.
- $\Omega(\text{drone}_i)$: Solid angle subtended by drone i at the observer.
- $\Omega(\text{open sky})$: Solid angle of open sky (without buildings).
- $\Omega(\text{urban})$: Solid angle occupied by urban objects.
- a_i: Area of drone i.
- R_i: Distance from observer to drone i.
- $atan(\frac{a_i}{R_i^2})$: Trigonometric estimation of the solid angle for each drone.

In practical case studies over Madrid, the VP-1 indicator showed that 45,125 people were able to see a drone during a single cruise flight, with the highest concentrations near the flight path. Applying a VPC threshold (VP-2) reduced the affected population to 750 people (AiRMOUR metric) and 659 people (visible area metric), demonstrating the importance of threshold selection. The VP-4 indicator (total exposure) further revealed that exposure was highest along the trajectory and in densely populated areas, with segmentation by age and gender providing additional insight into the distribution of visual impact [18].

3.3.2.2.2.3 Privacy Impact

In parallel, [10] defines a suite of quantitative privacy concern indicators (PC-1 to PC-5) to assess the impact of drone operations on perceived privacy: PC-1 and PC-2 measure the number of people visually annoyed by a single drone operation or exposed to hovering drones at close range; PC-3 and PC-4 extend these metrics to the area level, quantifying the total number of people annoyed or exposed to hovering drones within a given zone and time period; and PC-5 captures the accumulated duration of visual exposure to hovering drones for all affected individuals in an area. These indicators, expressed in units such as “person” or “person·vp·h”, are designed to reflect both the scale and intensity of privacy-related disturbance, enabling practical, context-sensitive evaluation and management of privacy impacts from UAS operations.

3.3.2.2.2.4 Emissions Impact

For emissions, [10] proposes five quantitative indicators (EM-1 to EM-5) to assess the environmental impact of drone operations: EM-1 measures the actual average CO_2 emissions per flight; EM-2 and EM-3 quantify energy consumption and CO_2-equivalent emissions for individual drone trajectories; EM-4 aggregates area-based CO_2-equivalent emissions over a given period; and EM-5 captures the reduction in area-based CO_2-equivalent emissions when drones replace conventional road deliveries.

3.3.2.2.2.5 Wildlife Impact

For wildlife, six indicators (WL-1 to WL-6) are defined to monitor the impact of drone traffic on animal populations: WL-1 and WL-2 measure the total amount of wildlife exposed to noise and visual disturbance along specific trajectories or within an area; WL-3 and WL-4 quantify the annoyance level for single trajectories or traffic scenarios; and WL-5 and WL-6 track changes in wildlife presence within noise or appearance contours over time [10].

3.3.2.2.2.6 Economic Impact

For economic impact, two indicators (EC-1 and EC-2) are introduced: EC-1 quantifies the area (in km²) experiencing positive economic influence, such as job creation, due to drone operations; EC-2 measures the area where property values decrease as a result of frequent drone activity [10].

3.3.2.2.2.7 Security Impact

The National Aeronautics and Space Administration (NASA) Control and Non-Payload Communications (CNPC) risk assessment methodology [19] recommends beginning with a thorough system characterisation, identifying all assets, information types, and operational functions relevant to the UAS.

EUROPEAN PARTNERSHIP

Co-funded by the European Union

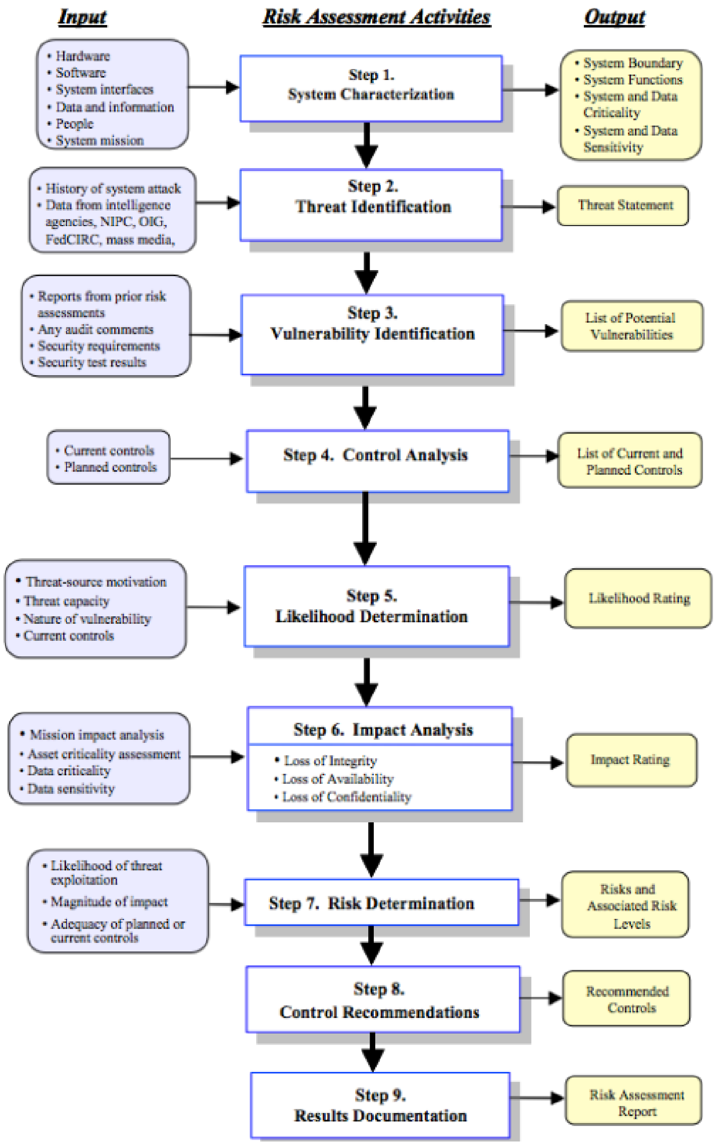

Figure 15 – Risk Assessment Methodology Flowchart [19].

Operators can then conduct a security categorisation, evaluating the potential severity from a loss of confidentiality, integrity, or availability for each information type. This security categorisation (SC) is expressed as a tuple for each information type:

$$\mathrm{SC} = \{(\mathrm{confidentiality, impact}), (\mathrm{integrity, impact}), (\mathrm{availability, impact})\}$$

The highest impact value across these determines the overall system categorisation, which then guides the selection of baseline security controls.

Building on knowledge graphs outlined in [20] operators can be guided to adopt scenario-based modelling that accounts for dynamic factors such as airspace density, communication vulnerabilities, potential cyber-physical threats, etc. This requires harmonising probabilistic risk assessment with real-time monitoring tools, enabling operators to calculate security impacts under varying operational conditions.

Threat identification is performed by considering all plausible threat sources, including cyber-attacks (e.g., hacking, jamming, spoofing, etc.), physical attacks, and insider threats [21]. Vulnerabilities are then identified by reviewing system design, operational procedures, and known weaknesses, referencing common vulnerabilities such as unencrypted communications, lack of authentication, or outdated firmware. For each threat-vulnerability pair, the operator determines the likelihood of exploitation and the potential impact, using standard definitions (e.g., High, Medium, Low) and numerical values. Likelihood and severity impact are then combined in a risk matrix to assign a risk rating to each scenario.

To calculate the expected annual cost of potential data breaches, operators use the formula [22]:

$$\mathrm{EB} = \sum_{i=1}^{n} (\mathrm{P}_i \times \mathrm{A}_i)$$

Where:

- P_i = Likelihood of data breach type.
- A_i = Total cost per breach for type.

Each scenario i is assigned a probability (based on likelihood and vulnerability) and an estimated impact (e.g., cost, downtime, reputational loss, etc.). The risk matrix and quantification worksheet are then used to prioritise mitigation actions, focusing on scenarios with the highest annualised risk or regulatory concern.

3.3.3 Weight Factors

3.3.3.1 Ground Impacts

For ground impacts, it is not appropriate to apply weight factors, as the underlying methodology is based on research focused specifically on airborne activities such as delivery drones and air taxis. Since ground impacts are not addressed or quantified within this research, there is insufficient data to establish reasonable or meaningful weightings for these indicators. Accordingly, assigning normalized weights to ground impacts would lack empirical support and does not align with the evidence-based approach adopted in this framework.

3.3.3.2 Other-than-Ground Impacts

The EASA survey results [23] show respondents' top concerns for delivery drones and air taxis.

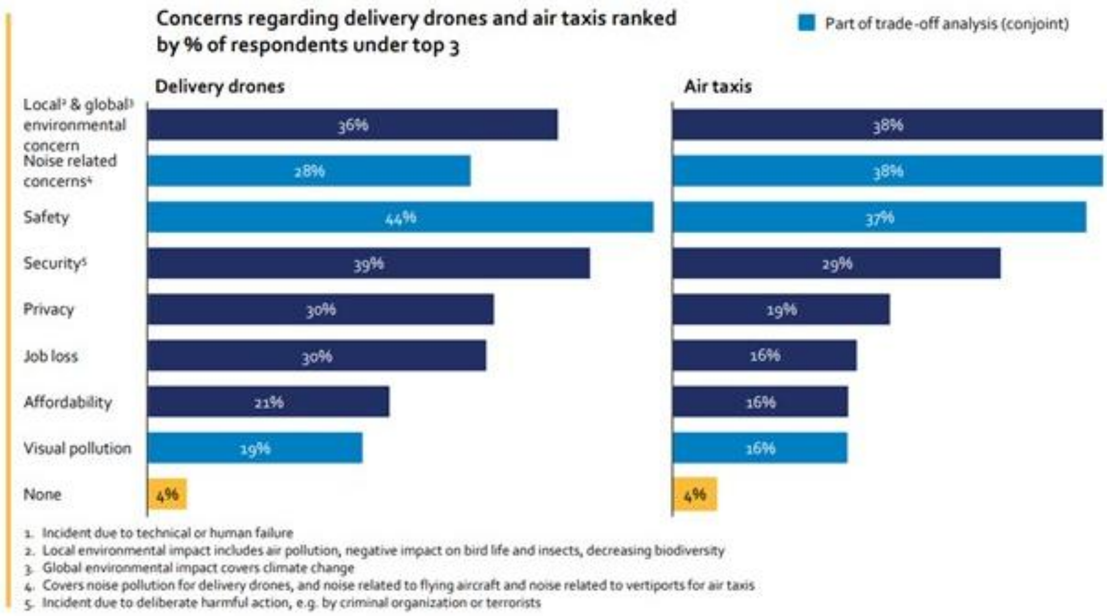

Figure 16 – Respondents' concerns about delivery drones and air taxis [23].

These concerns were mapped to the indicators as follows:

- Local and Global Environmental Concerns → Emissions Impact + Wildlife Impact.
- Noise-Related Concerns → Noise Impact.
- Security → Security Impact.
- Privacy → Privacy Impact.
- Job Loss → Economic Impact.
- Visual Pollution → Visual Pollution Impact.

Next, we aggregated the percentages for each mapped indicator based on the survey results. For delivery drones, the values were: Emissions/Wildlife (36%), Noise (28%), Security (39%), Privacy (30%), Economic (30%), and Visual Pollution (19%). For air taxis, the values were: Emissions/Wildlife (38%), Noise (38%), Security (29%), Privacy (19%), Economic (16%), and Visual Pollution (16%).

To ensure comparability, each indicator's percentage was converted into weight factors. Thus, for delivery drones, the weights are described below.

Delivery Drones	
Performance Indicator Domain	**Weight Factor**
Noise Impact	0.28
Visual Pollution Impact	0.19
Privacy Impact	0.3
Emissions/Wildlife Impact	0.36

Co-funded by the European Union

Delivery Drones	
Performance Indicator Domain	**Weight Factor**
Economic Impact	0.3
Security Impact	0.39

Table 21: Weight factors assignment for performance indicator domains of delivery drones.

The results highlight different priorities for each category. For delivery drones, security and emissions/wildlife Impacts are the most significant concerns, followed by privacy and economic impacts. Noise impact is slightly lower, and visual pollution ranks last.

For air taxis, the weights are described below.

Air Taxis	
Performance Indicator Domain	**Weight Factor**
Noise Impact	0.38
Visual Pollution Impact	0.16
Privacy Impact	0.19
Emissions/Wildlife Impact	0.38
Economic Impact	0.16
Security Impact	0.29

Table 22: Weight factors assignment for performance indicator domains of air taxis.

For air taxis, noise and emissions/wildlife impacts dominate equally, with security next. Privacy and economic impacts are less critical, and visual pollution remains the lowest concern.

3.3.4 Composite Score

The final composite severity score is a weighted sum of the scores assigned to each negative effect factor (performance indicator domain), such as noise pollution, visual pollution, privacy concerns, emissions, wildlife impact, and economic impact. Each factor is scored (low-high or 0–2) based on its severity obtained from section 3.3.2.2.1, then multiplied by its assigned weight from section 3.3.3.2 (reflecting its relevance for the public), and all weighted scores are summed.

$$Composite\ Score = \sum (Weight\ Factor\ \times Severity\ Score)$$

Composite Score	Level	Meaning
< 1	Low	Negligible or minor negative impact across all domains.

1 – 2	Medium	Some negative impact present; may approach or slightly exceed thresholds in one or more factors.
> 2	High	Significant to severe negative impact; thresholds exceeded in multiple factors or far exceed acceptable limits.

Table 23: Composite score assignment for performance indicator domains of delivery drones and air taxis.

Numerical implementation for assessing the severity of negative effects, both for ground impacts and other types, are provided below as examples for implementation.

3.3.5 Numerical implementation

3.3.5.1 Ground Impacts

The following scenarios apply the qualitative severity scale defined in 3.3.2.1.1, using the severity levels and meanings specified in Table 18: Severity score for negative effects related to ground impacts.

Severity scores (High = 2, Medium = 1, Low = 0) are assigned consistently across the environmental, economic, and reputational domains, considering only external impacts, as required by the methodology.

3.3.5.1.1 Scenario 1 – Crash in a suburban residential area (rooftop impact)

This scenario considers a drone crash in a suburban residential environment, involving impact on a building rooftop. The area is not classified as highly sensitive (e.g. national park), but it includes residential dwellings and exposed third-party property. The crash causes a battery fire, visible smoke, and noise, with no chemical spill.

Factor	Level	Score	Meaning
Environmental	High	2	The crash occurs in a populated residential area and causes severe noise and visible pollution (smoke/fire), affecting people in the immediate vicinity.
Economic	High	2	The crash causes significant financial damage to third-party property (rooftop equipment, solar panels) and temporary building closure.
Reputational	Medium	1	The incident generates local media coverage

Factor	Level	Score	Meaning
			and temporary stakeholder concern, without long-term trust damage or widespread scrutiny.

Table 24: Severity score from ground impacts for scenario 1.

Scenario 1 represents a high-severity ground-impact event, driven primarily by environmental disturbance and significant third-party economic damage in a residential context. Reputational effects remain limited to the local level.

3.3.5.1.2 Scenario 2 – Crash on a suburban roadway (low traffic)

This scenario examines a drone crash on a suburban road with low traffic volume. The surrounding area is not environmentally sensitive. The crash causes debris on the road, brief noise disturbance, and damage to a parked vehicle, without hazardous material release.

Factor	Level	Score	Meaning
Environmental	Medium	1	The crash causes noticeable but localized pollution (noise and debris) near a road, with moderate exposure and no sensitive environments affected.
Economic	Medium	1	Damage is limited to minor third-party property damage (parked car) and minor traffic disruption, consistent with Medium economic severity (“minor damage to private property or public infrastructure”).
Reputational	Low	0	The incident receives no media attention and is handled through insurance.

Table 25: Severity score from ground impacts for scenario 2.

Scenario 2 corresponds to a medium-severity ground-impact event, where impacts are tangible but limited in scope and duration, and do not escalate beyond the immediate area.

EUROPEAN PARTNERSHIP
Co-funded by the European Union

3.3.5.1.3 Scenario 3 – Crash in a rural or agricultural area

This scenario considers a drone crash in a rural farmland setting, occurring in an open field away from residential areas, public infrastructure, and environmentally sensitive zones. The crash results in minimal noise and negligible crop damage.

Factor	Level	Score	Meaning
Environmental	Low	0	The crash occurs in a remote area, with minimal pollution and no people affected.
Economic	Low	0	There is no material third-party financial damage, aside from negligible crop impact.
Reputational	Low	0	The incident generates no public awareness or media coverage.

Table 26: Severity score from ground impacts for scenario 3.

Scenario 3 represents a low-severity ground-impact event, illustrating how low population density and absence of exposed assets significantly limit negative effects across all domains.

3.3.5.2 Other-than-Ground Impacts

The following scenarios apply the qualitative severity levels defined in Table 20: Severity score for negative effects related to other-than-ground impacts. for other-than-ground impacts. Severity scores (High = 2, Medium = 1, Low = 0) are assigned consistently across the operational domains listed in 3.3.1.2.

In accordance with 3.3.3.2 and 3.3.4, weight factors derived from the EASA societal-acceptance study are applied to compute an overall (composite) severity score for each scenario.

3.3.5.2.1 Scenario 4 – Infrastructure inspection in a suburban environment

This scenario considers a drone mission for bridge and powerline inspection along a linear corridor of approximately 3 km in a suburban area with moderate population density (≈500 people/km²). Operations are conducted during daytime using an electric drone, with limited flight duration and low repetition rate.

Factor	Level	Score	Meaning
Noise Impact	Medium	1	Operations cause noticeable noise disturbance, leading to moderate annoyance for residents near the corridor.

Factor	Level	Score	Meaning
Visual Pollution Impact	Medium	1	The drone is visible to pedestrians and drivers along the route, exposing a moderate number of people.
Privacy Impact	Medium	1	Flights occur near residential areas with moderate privacy requirements (e.g. villa districts).
Emissions/Wildlife Impact	Low	0	The drone is fully electric and emissions remain below regulatory limits. No sensitive habitats are present; wildlife disturbance is negligible.
Economic Impact	Low	0	No measurable effects on jobs, property values, or businesses.
Security Impact	Low	0	Operations take place in suburban areas with robust security measures and no sensitive data transmission.

Table 27: Severity score from other-than-ground impacts for scenario 4.

Applying the weight factors yields a composite score of 0.77, corresponding to a low overall severity effect.

Factor	Composite Score Calculation
Noise Impact	0.28
Visual Pollution Impact	0.19
Privacy Impact	0.3
Emissions/Wildlife Impact	0
Economic Impact	0
Security Impact	0

Factor	Composite Score Calculation
Composite Score	**0.77 (low severity effect)**

Table 28: Composite severity score from other-than-ground impacts for scenario 4.

This scenario shows that limited exposure, short duration, and controlled operations keep societal impacts low despite moderate effects across multiple domains.

3.3.5.2.2 Scenario 5 – Delivery operations in a dense urban centre

This scenario evaluates delivery drone operations in a dense urban centre with population density exceeding 5,000 people/km². The flight path crosses crowded streets, commercial venues, schools, and hospitals, with high operational frequency and strong public visibility.

Factor	Level	Score	Meaning
Noise Impact	High	2	Continuous operations cause severe noise disturbance and widespread annoyance in densely populated areas.
Visual Pollution Impact	High	2	Drones are highly visible in crowded public spaces, causing strong visual disturbance.
Privacy Impact	High	2	Operations occur near sensitive venues (schools, hospitals), leading to strong privacy concerns.
Emissions/Wildlife Impact	Low	0	Fully electric operation results in negligible emissions. Urban environment with no sensitive habitats.
Economic Impact	Medium	1	Operations may cause some negative economic effects, such as disruption to businesses or delivery services.
Security Impact	High	2	Proximity to critical infrastructure increases

Factor	Level	Score	Meaning
			the consequences of potential interception or misuse.

Table 29: Severity score from other-than-ground impacts for scenario 5.

The weighted aggregation results in a composite score of 2.62, classified as a high severity effect.

Factor	Composite Score Calculation
Noise Impact	0.56
Visual Pollution Impact	0.38
Privacy Impact	0.6
Emissions/Wildlife Impact	0
Economic Impact	0.3
Security Impact	0.78
Composite Score	**2.62 (high severity effect)**

Table 30: Composite severity score from other-than-ground impacts for scenario 5.

This scenario highlights how population density, sensitivity of the environment, and cumulative exposure dominate the overall societal impact of urban delivery operations.

3.3.5.2.3 Scenario 6 – Operations over a national park or protected natural area

This scenario considers drone operations conducted over or near a national park or protected natural area, characterised by very low human population density but high environmental sensitivity. Operations may include environmental monitoring, mapping, or surveillance flights. The area hosts protected habitats and wildlife species, and flights are conducted at low frequency using electric drones.

Factor	Level	Score	Meaning
Noise Impact	Low	0	Human exposure is negligible, as the area is remote and sparsely populated.
Visual Pollution Impact	Low	0	Visual exposure affects very few people, limited mainly to park staff or occasional visitors.
Privacy Impact	Low	0	The area has no specific privacy protection

Co-funded by the European Union

Factor	Level	Score	Meaning
			requirements (no residential or sensitive human venues).
Emissions/Wildlife Impact	High	2	Electric propulsion results in negligible emissions, well below regulatory limits. Operations occur in or near sensitive habitats and may cause significant disturbance to protected wildlife.
Economic Impact	Low	0	No measurable impact on jobs, property values, or commercial activity.
Security Impact	Low	0	Operations do not involve sensitive data or critical infrastructure, and are conducted with robust security measures.

Table 31: Severity score from other-than-ground impacts for scenario 6.

The weighted aggregation results in a composite score of 0.72, classified as a low severity effect.

Factor	Composite Score Calculation
Noise Impact	0
Visual Pollution Impact	0
Privacy Impact	0
Emissions/Wildlife Impact	0.72
Economic Impact	0
Security Impact	0
Composite Score	**0.72 (low severity effect)**

Table 32: Composite severity score from other-than-ground impacts for scenario 6.

Although the overall composite severity remains low due to minimal human exposure, this scenario highlights that environmental sensitivity, particularly wildlife disturbance, can be the dominant impact

Co-funded by the European Union

driver in protected natural areas. This underscores the need for specific operational constraints and mitigations when operating in environmentally sensitive contexts.

In conclusion, all these scenarios provide guidance to support UAS operators in conducting a detailed assessment of the severity of negative effects of UAS operations for ground impacts and other than ground impacts. It enables UAS operators to systematically assess and communicate qualitatively the severity of negative effects from their operations.

4 References

[1] ‘UAS Ground Collision Severity Evaluation’. FAA UAS Center of Excellence Task A4, Apr. 28, 2017.
[2] ‘Initial Ground Risk Model, U-AGREE Project, Deliverable D3.2, Edition 01.00’. SESAR JU, 2025.
[3] ‘Modelling Unmanned Aerial System (UAS) Risks via Monte Carlo Simulation’, E. Rudnick-Cohen, J. W. Herrmann, S. Azarm, International Conference on Unmanned Aircraft Systems, 2019.
[4] Annex to ED Decision 2025/018/R ‘AMC and GM to Regulation (EU) 2019/947 — Issue 1, Amendment 3’.
[5] SORA v. 2.5, Annex F – “Theoretical Basis for Ground Risk Classification and Mitigation”. JARUS, 2024.
[6] Anders la Cour-Harbo. Ground impact probability distribution for small unmanned aircraft in ballistic descent. In 2020 International Conference on Unmanned Aircraft Systems (ICUAS), 1442–1451. Aalborg University, IEEE, sep 2020. doi:10.1109/ICUAS48674.2020.9213990.
[7] SORA v. 2.5, Main body – “JARUS guidelines on Specific Operations Risk Assessment (SORA)”. JARUS, 2024.
[8] Sun, J., & Hubbard, S. (2025). An Examination of UAS Incidents: Characteristics and Safety Considerations. Drones, 9(1), 112.
[9] Dalamagkidis, K., Valavanis, K. P., & Piegl, L. A. (2008). Evaluating the Risk of Unmanned Aircraft Ground Impacts. Proceedings of the 16th Mediterranean Conference on Control and Automation, Ajaccio, France, June 25–27, 2008, pp. 709–716.
[10] Krstić Simić, T., Ganić, E., Mirković, B., Baena, M., LeGriffon, I., & Barrado, C. (2025). U-Space Social and Environmental Performance Indicators. Drones, 9(1), 113.
[11] T. Randall, “Noise Impact Assessment.” [Online]. Available: https://vibrationdata.com/tutorials/Noise_Impact_Assessment.pdf. [Accessed: 03-Dec-2025]]
[12]Susini, A. (2025). A Technocritical Review of Drones Crash Risk: Probabilistic Consequences and its Societal Acceptance. Deutsche Gesellschaft für Kartographie (DGfK) – Risk Commission Member, Versoix, Switzerland.
[13] Wang, H., Ye, B., Qu, X., & Wan, L. (2025). Research on Risk Map Based on UAV Safety Operation Indicators. Nanjing University of Aeronautics and Astronautics, Nanjing, Jiangsu, China.
[14] Alcaide, M. Á., Celani, A., Cervera Chasan, P., & De La Poza, E. (2022). Mathematical Modeling of the Financial Impact of Air Crashes on Airlines and Involved Manufacturers. Mathematics, 10(5), 715.
[15] Bougias, A. (2019). Impact of Airplane Crashes on Firm's Credit Risk Under the CreditGrades Model. Undergraduate Economic Review, 15(1), Article 6. Available: https://digitalcommons.iwu.edu/uer/vol15/iss1/6/. [Accessed: 03-Dec-2025]
[16] Spaltro, A. (2018). [Title of the thesis] (bachelor’s thesis). LUISS Guido Carli University, Rome, Italy. Retrieved from https://tesi.luiss.it/23524/1/682391_SPALTRO_ANDREA_Thesis%20Andrea%20Spaltro%20682391.pdf. [Accessed: 03-Dec-2025]]
[17] Collings, D., Corbet, S., Hou, Y., Hu, Y., Larkin, C., & Oxley, L. (2022). The effects of negative reputational contagion on international airlines: The case of the Boeing 737-MAX disasters. International Review of Financial Analysis, 82, 102103.
[18] Baena, M., Alonso, M., Mocholí, D., LeGriffon, I., Ruaud, E., Barrado, C., Ganić, E., & Krstić Simić, T. (2024). A Methodology for Evaluating UAM Noise and Visual Pollution. In Proceedings of the SIDs 2024 Conference

[19] Iannicca, D. C., Young, D. P., Thadhani, S. K., & Winter, G. A. (2013). SECURITY RISK ASSESSMENT PROCESS FOR UAS IN THE NAS CNPC ARCHITECTURE. NASA Glenn Research Center, DB Consulting Group, Inc., Verizon Federal Network Systems, Cleveland, Ohio]

[20] Zhang, Y., Wang, J., & Li, X. (2023). Security Risk Assessment for Unmanned Aerial Systems: A Probabilistic Approach.

[21] U.S. Department of Homeland Security, Cybersecurity and Infrastructure Security Agency, Interagency Security Committee. (2020). Protecting against the threat of unmanned aircraft systems (UAS): An Interagency Security Committee best practice (November 2020 edition)]

[22] Khan, M. A., & Salah, K. (2021). IoT Security: Review, Blockchain Solutions, and Open Challenges. Applied Sciences, 11(8), 3678.

[23] European Union Aviation Safety Agency (EASA), & McKinsey & Company. (2021). Study on the societal acceptance of Urban Air Mobility in Europe. https://www.easa.europa.eu/UAM]

[24] https://moduliweb.enac.gov.it/applicazioni/SAPR/APR_Lista_Unificata.asp

[25] Proposed Amendments to UK Acceptable Means of Compliance and Guidance Material for UK Regulation (EU) 2019/945 and 2019/947, September 2025

[26]https://episcope.eu/welcome/

[27]Eurostat (2025) Housing in Europe — 2025 edition https://ec.europa.eu/eurostat/web/interactive-publications/housing-2025, [Accessed: 09-apr-2026].

[28]https://webtool.building-typology.eu/#bm

Appendix A

A.1 Aircraft data used to model Monte Carlo simulation parameters

Appendix A.1 provides a summary of the input data and reference parameters used to support the Monte Carlo simulations described in the main body of the document. The data are derived from publicly available aircraft documentation (e.g. flight manuals and datasheets) and are intended to support the definition of representative performance envelopes for different UAS categories.

Aircraft Model	MTOM [kg]	Vx [m/s] (groundspeed)	Vy [m/s]
DJI Agras T100	175	26	3
DJI Agras T50	103	16	3
DJI Agras T25	58	16	3
DJI FlyCart 30	95	32	5
Flying Basket FB3	115	30	5
DJI Agras T30	76.5	13	Not Available
X6000 Pro+ RTK	32	15	4
TALOS T60X	125	19.8	Not available

Table 33: Aircraft characteristics and maximum speed values for multirotor UAS

Aircraft Model	MTOM [kg]	Max V [m/s] (groundspeed)
Elytron Talisman	50	43
Shield AI V-BAT	73	25
TEKEVER AR5	150	28
Rigitech ER-03	21	47
Germandrones Songbird	14	34
Milvus Tesi S.r.l.	65	45
Aertec Solutions	75	28
FoxTech Ayk 350	35	40

Table 34: Maximum speed values for selected fixed-wing UAS

A.2 Simulation results

Appendix A2 provides a comprehensive compilation of the simulation results obtained from the case study described in section 3.1.3 (assessing sheltering for UAS with MTOM>25 kg). These results, which were previously presented in graphical format, are now detailed in this appendix for reference and further analysis.

A.2.1 Case study 1

Mass	Nr. of trials	Probability of no penetration	50th Percentile aircraft kinetic energy [J]	50th Percentile energy absorbed by the building [J]	50th Percentile Net KE [J]
5	**1000**	0.974	971.0	772516.8	-771503.3
	10000	0.975	958.4	744153.3	-742946.9
	100000	0.97511	954.8	750943.4	-749833.3
10	**1000**	0.937	3085.0	772516.8	-769572.4
	10000	0.9303	3114.3	744153.3	-740718.8
	100000	0.92959	3106.0	750943.4	-747408.7
10	**1000**	0.937	3085.0	772516.8	-769572.4
	10000	0.9303	3114.3	744153.3	-740718.8
	100000	0.92959	3106.0	750943.4	-747408.7
15	**1000**	0.904	5826.7	772516.8	-767149.4
	10000	0.9048	5852.3	744153.3	-737520.2
	100000	0.90496	5856.6	750943.4	-744538.4
20	**1000**	0.901	8960.6	772516.8	-764695.4
	10000	0.901	8924.6	744153.3	-734101.5
	100000	0.90145	8979.0	750943.4	-741144.4
	100000	0.90145	8979.0	750943.4	-741144.4
25	**1000**	0.901	12254.0	772516.8	-762566.7
	10000	0.9001	12291.4	744153.3	-730943.2
	100000	0.90066	12363.1	750943.4	-737523.7

50	**1000**	0.901	31114.2	772516.8	-743782.2
	10000	0.8994	31038.3	744153.3	-712714.4
	100000	0.9	31066.4	750943.4	-719201.8
75	**1000**	0.901	50878.7	772516.8	-722558.5
	10000	0.8994	50847.3	744153.3	-692264.5
	100000	0.89997	50651.2	750943.4	-700662.2
100	**1000**	0.901	70686.5	772516.8	-705820.2
	10000	0.8994	70365.7	744153.3	-673808.9
	100000	0.89997	70235.7	750943.4	-681209.6
125	**1000**	0.901	90610.3	772516.8	-690568.1
	10000	0.8994	90108.3	744153.3	-655011.9
	100000	0.89997	89838.1	750943.4	-661441.5
150	**1000**	0.901	110409.6	772516.8	-669344.1
	10000	0.8994	109842.5	744153.3	-636815.2
	100000	0.89997	109422.2	750943.4	-641852.3
175	**1000**	0.901	130035.9	772516.8	-646437.0
	10000	0.8994	129528.5	744153.3	-616655.0
	100000	0.89997	129049.2	750943.4	-621868.6
200	**1000**	0.901	149616.2	772516.8	-625740.5
	10000	0.8993	149157.7	744153.3	-597661.2
	100000	0.89951	148664.4	750943.4	-602720.2

Table 35 - Sheltering case study 1 results

A.2.2 Case study 2

Mass	**Nr. of trials**	**Probability of no penetration**	**50th Percentile aircraft kinetic energy [J]**	**50th Percentile energy absorbed by the building [J]**	**50th Percentile Net KE [J]**
5	**1000**	0.924	1953.0	718978.0	-716015.0

	10000	0.9192	2008.6	731956.4	-729301.3
	100000	0.92326	2009.7	722446.7	-719932.3
10	**1000**	0.879	3906.0	718978.0	-713855.5
	10000	0.877	4017.2	731956.4	-727196.2
	100000	0.87935	4019.4	722446.7	-717538.6
15	**1000**	0.861	5859.0	718978.0	-712443.6
	10000	0.8633	6025.8	731956.4	-724811.1
	100000	0.86606	6029.2	722446.7	-715121.9
20	**1000**	0.856	7812.0	718978.0	-710316.0
	10000	0.8588	8034.4	731956.4	-722396.5
	100000	0.86096	8038.9	722446.7	-712795.9
25	**1000**	0.855	9765.0	718978.0	-708340.9
	10000	0.8574	10043.0	731956.4	-719955.1
	100000	0.85952	10048.6	722446.7	-710632.2
50	**1000**	0.854	19530.0	718978.0	-696159.1
	10000	0.8573	20085.9	731956.4	-706215.5
	100000	0.85949	20097.2	722446.7	-698876.3
75	**1000**	0.854	29295.0	718978.0	-683810.2
	10000	0.8573	30128.9	731956.4	-694752.6
	100000	0.85949	30145.9	722446.7	-686780.1
100	**1000**	0.854	39060.0	718978.0	-666823.6
	10000	0.8573	40171.9	731956.4	-683341.2
	100000	0.85949	40194.5	722446.7	-675012.8
125	**1000**	0.854	48825.0	718978.0	-652313.8
	10000	0.8573	50214.8	731956.4	-671215.8
	100000	0.85949	50243.1	722446.7	-663052.6

EUROPEAN PARTNERSHIP
Co-funded by the European Union

150	**1000**	0.854	58590.0	718978.0	-641561.7
	10000	0.8573	60257.8	731956.4	-658655.5
	100000	0.85949	60291.7	722446.7	-651197.2
175	**1000**	0.854	68355.0	718978.0	-632248.3
	10000	0.8573	70300.8	731956.4	-646398.4
	100000	0.85949	70340.4	722446.7	-639255.2
200	**1000**	0.854	78120.0	718978.0	-619816.4
	10000	0.8573	80343.7	731956.4	-632917.1
	100000	0.85949	80389.0	722446.7	-627836.4

Table 36 - Sheltering case study 2 results

A.2.3 Case study 3

Mass	**Nr. of trials**	**Probability of no penetration**	**50th Percentile aircraft kinetic energy [J]**	**50th Percentile energy absorbed by the building [J]**	**50th Percentile Net KE [J]**
5	**1000**	0.972	1099.0	745644.3	-744531.2
	10000	0.9661	1107.7	733150.4	-731781.2
	100000	0.96645	1098.3	746846.7	-745624.4
10	**1000**	0.922	3357.4	745644.3	-742790.6
	10000	0.9164	3419.5	733150.4	-729175.7
	100000	0.91678	3401.4	746846.7	-742982.2
15	**1000**	0.895	6149.9	745644.3	-740647.8
	10000	0.894	6258.5	733150.4	-726286.5
	100000	0.89282	6226.1	746846.7	-740050.1
20	**1000**	0.89	9360.1	745644.3	-738046.1
	10000	0.8911	9401.8	733150.4	-723018.5
	100000	0.89037	9392.1	746846.7	-736620.2
25	**1000**	0.89	12866.2	745644.3	-733893.7

Co-funded by the European Union

	10000	0.8908	12866.7	733150.4	-719649.3
	100000	0.89001	12874.5	746846.7	-732951.6
50	**1000**	0.89	31683.6	745644.3	-714310.7
	10000	0.8908	32110.9	733150.4	-698774.5
	100000	0.89	32236.0	746846.7	-713723.5
75	**1000**	0.89	52581.2	745644.3	-688045.9
	10000	0.8908	52315.3	733150.4	-678899.9
	100000	0.89	52553.1	746846.7	-694142.1
100	**1000**	0.89	72484.4	745644.3	-667647.5
	10000	0.8908	72509.5	733150.4	-659089.7
	100000	0.89	72773.7	746846.7	-673896.1
125	**1000**	0.89	93151.2	745644.3	-646664.7
	10000	0.8908	92807.2	733150.4	-638738.9
	100000	0.89	93002.6	746846.7	-653535.5
150	**1000**	0.89	113741.6	745644.3	-632718.1
	10000	0.8908	112906.2	733150.4	-619877.8
	100000	0.89	113320.6	746846.7	-632290.7
175	**1000**	0.89	134254.9	745644.3	-612476.9
	10000	0.8908	133110.6	733150.4	-600098.6
	100000	0.88993	133575.2	746846.7	-612013.9
200	**1000**	0.889	154353.1	745644.3	-597396.1
	10000	0.8893	153324.6	733150.4	-579731.9
	100000	0.8889	153879.9	746846.7	-591148.9

Table 37 - Sheltering case study 3 results